Journal of Medicinal Chemistry

Article

Design and Synthesis of Brain Penetrant Trypanocidal *N*-Myristoyltransferase Inhibitors

Tracy Bayliss, David A. Robinson, Victoria C. Smith, Stephen Brand, Stuart P McElroy, Leah S. Torrie, Chido Mpamhanga, Suzanne Norval, Laste Stojanovski, Ruth Brenk, Julie A Frearson, Kevin D Read, Ian H. Gilbert, and Paul G. Wyatt

J. Med. Chem., **Just Accepted Manuscript** • DOI: 10.1021/acs.jmedchem.7b01255 • Publication Date (Web): 10 Nov 2017

ACS Publications

Journal of Medicinal Chemistry is published by the American Chemical Society. 1155 Sixteenth Street N.W., Washington, DC 20036

Design and Synthesis of Brain Penetrant Trypanocidal *N*-Myristoyltransferase Inhibitors

Tracy Bayliss, David A. Robinson, Victoria C. Smith, Stephen Brand, Stuart P. McElroy, Leah S. Torrie, Chido Mpamhanga, Suzanne Norval, Laste Stojanovski, Ruth Brenk, Julie A. Frearson, Kevin D. Read, Ian H. Gilbert, Paul G. Wyatt.*

Drug Discovery Unit, College of Life Sciences, University of Dundee, Sir James Black Centre, Dundee, DD1 5EH, UK.

ABSTRACT: *N*-Myristoyltransferase (NMT) represents a promising drug target within the parasitic protozoa *Trpanosoma brucei (T. brucei)*, the causative agent for human African trypanosomiasis (HAT) or sleeping sickness. We have previously validated *T. brucei* NMT as a promising druggable target for the treatment of HAT in both stage 1 and 2 of the disease. We report on the use of the previously reported DDD85646 (**1**) as a start point for the design of a class of potent, brain penetrant inhibitors of *T. brucei* NMT.

INTRODUCTION

Human African trypanosomiasis (HAT) or sleeping sickness is prevalent in sub-Saharan Africa[1] with an estimated "at risk" population of 65 million[2]. The causative agents of HAT are the protozoan parasites *Trypanosoma brucei gambiense* and *Trypanosoma brucei rhodesiense*[3-4] transmitted through the bite of an infected tsetse fly. HAT progresses through two stages. In the first stage (stage 1), the parasites proliferate solely within the bloodstream.

In the second, late stage (stage 2), the parasite infects the central nervous system (CNS) causing the symptoms characteristic of the disease, such as disturbed sleep patterns and often death[5]. Currently there are a number of treatments available for HAT, though none are without issues, including toxicity and inappropriate routes of administration for a disease of rural Africa[6].

Research has revealed enzymes and pathways that are crucial for the survival of *T. brucei*, and based on these studies, a number of anti-parasitic drug targets have been proposed[7-10]. *T. brucei N*-myristoyltransferase (*Tb*NMT) is one of the few *T. brucei* druggable targets to be genetically and chemically validated in both *in vitro* and in rodent models of HAT[7, 11-12]. NMT is a ubiquitous essential enzyme in all eukaryotic cells. It catalyses the co- and post-translational transfer of myristic acid from myristoyl-CoA to the N-terminal glycine of a variety of peptides. Protein N-myristoylation facilitates membrane localization and biological activity of many important proteins[11, 13].

NMT has been extensively investigated as a potential target for the treatment of other parasitic diseases including malaria[14], leishmaniasis[15] and Chagas' disease[16-17] resulting in the identification of multiple chemically distinct small molecule inhibitors[18]. NMT has also been shown to be a potential therapeutic target for human diseases such as autoimmune disorders [19] and cancer[20-21].

Previously we have reported the discovery of compound **1** (Figure 1)[7, 22-23] which showed excellent levels of inhibitory potency for *Tb*NMT and *T. brucei brucei* (*T. br. brucei*) proliferation *in vitro* and was used as a model compound to validate *Tb*NMT as a druggable target for stage 1 HAT[7, 22]. However, **1** is not blood-brain barrier penetrant, a requirement for stage 2 activity. Two approaches were taken to increase the brain penetration of **1**. A classical

lead optimisation approach is described elsewhere[24]. This paper describes a second approach that used a minimum pharmacophore of **1** aiming to derive a structurally distinct series of potent *Tb*NMT inhibitors with brain penetration, as leads for the identification of suitable candidates for the treatment of stage 2 HAT.

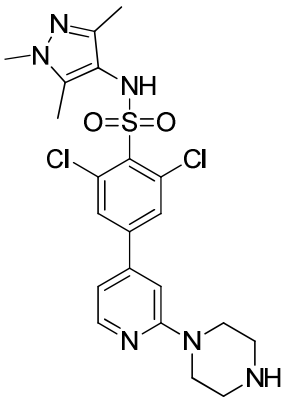

1: DDD85646
*Tb*NMT, IC_{50} 0.002 μM*
*Hs*NMT1, IC_{50} 0.004 μM*
T. br. brucei, EC_{50} 0.002 μM
MRC-5, EC_{50} 0.4 μM
Cint (mouse) 0.6 ml/min/g
Brain : Blood < 0.1
PSA 101Å^{2} [a]
Molecular weight 495[a]
LE 0.36[b]
Enzyme Selectivity = 2[c]

Figure 1. Compound **1**[a] *Potencies were determined against recombinant *Tb*NMT and *Hs*NMT1, and against bloodstream form *T. brucei brucei (T. br. brucei)* and MRC-5 proliferation studies *in vitro* using 10 point curves replicated ≥ 2. [a]Calculated using Optibrium STARDROP™ software. [b]Ligand efficiency (LE), calculated as 0.6*ln(IC_{50})/(heavy atom count) using *T. brucei* NMT IC_{50} potency[25]. IC_{50} values are shown as mean values of two or more determinations. Standard deviation was typically within 2-fold from the IC_{50}. [c]Enzyme selectivity calculated as *Hs*NMT1 IC_{50} (μM)/ *Tb*NMT IC_{50} (μM).

COMPOUND RATIONALE AND DESIGN

To aid compound design, and to significantly lower molecular weight and polar surface area (PSA), the chlorines and the sulfonamide moieties of **1** were removed to define a minimum pharmacophoric scaffold (Figure 2 panel A). This scaffold was chosen because the piperidine makes a key interaction through the formation of a salt bridge with NMT's terminal carboxylate.[10] This interaction is highly conserved across the binding modes of

NMT inhibitors covering multiple chemotypes including **1** (Figure 2 panel B) ; known anti-fungal NMT inhibitors such as Roche's (2-benzofurancarboxylic acid, 3-methyl-4-[3-[(3-pyridinylmethyl)amino]propoxy]-ethyl ester (RO-09-4609)[26-27], Searle's *N*-[2-[4-[4-(2-methyl-1*H*-imidazol-1-yl)butyl]phenyl]acetyl]-L-seryl-*N*-(2-cyclohexylethyl)- L-lysinamide, (SC-58272)[28] (Figure 2 panel C) and Pfizer's 2-((1r,4r)-4-(aminomethyl)cyclohexanecarboxamido)-N,N-dimethylbenzo[d]thiazole-6-carboxamide (UK-370,485)[29]. Attempts to crystallize *Tb*NMT had proved to be unsuccessful therefore, the fungal *Aspergillus fumigatus* NMT (*Af*NMT)[24, 30] were used as a surrogate model for *Tb*NMT in this study. *Af*NMT is 42% identical to *Tb*NMT, however within the peptide binding groove the level of identity is 92%. Previously, a selection of molecules from series **1** were assayed against *Af*NMT and *Tb*NMT using the SPA biochemical assay and pIC_{50} values compared using linear regression analysis. The pIC_{50} values were shown to be correlated with an R-squared value of 0.73 suggesting that *Af*NMT is a suitable surrogate system for study within this chemical series (see Supporting Information).

This minimum pharmacophoric scaffold had low molecular weight (237) and low PSA (12 $Å^2$ to maximise the potential for CNS penetration) from which we could design varied chemistry (Figure 2 panel A) to either access the serine pocket (occupied by the pyrazole moiety in **1**) or the peptide recognition region, as seen in the peptomimetic compound highlighted in red (Figure 2 panel C).

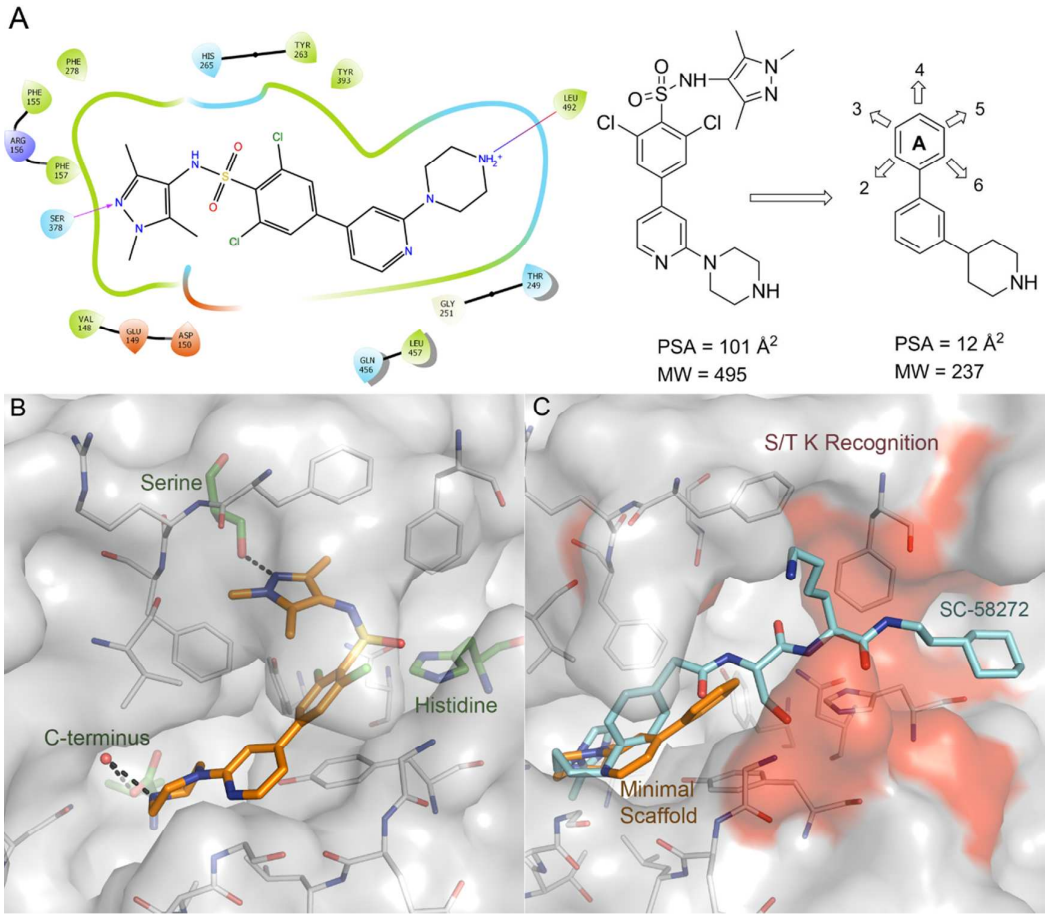

Figure 2. Development of the chemistry scaffold. A) 2D interaction map of **1** bound to *Af*NMT leading to the design of the minimal scaffold. B) Crystal structure of **1** bound; key recognition residues are highlighted and labelled. C) Proposed minimal scaffold (C atoms gold) docked into the crystal structure of *Af*NMT overlaid with peptomimetic compound PDB 2NMT (C atoms cyan); the key S/T K peptide recognition region is highlighted red.

Compound design. The adopted compound design strategy covered both compounds based on **1** (where common sulfonamide bioisosteres[31] and pyrazole mimics were included) and compounds based on the binding pocket structural features, probing these with diverse hydrogen bond acceptor (HBA) and hydrogen bond donor (HBD) groups. We employed high throughput chemistry, using technologies and techniques such as scavengers and solid supported reagents enabling arrays to be made in parallel. Three different but complementary

chemistries of Suzuki couplings, amidations and Mitsunobu reactions were chosen to explore all positions around ring A (Figure 3).

Crossing the blood-brain barrier (BBB) was an essential part our chemistry design and presented its own challenges. Improving the BBB permeation of molecules have been widely studied and *in silico* prediction methods developed based on known CNS penetrant and non-penetrant compounds[32-33]. Examination of the physicochemical properties of molecules and their influence on affecting BBB permeability has suggested some guiding principles and a physicochemical property range to increase the probability of improving the BBB permeability[33]. The top 25% CNS penetrant drugs sold in 2004 were found to have mean values of PSA ($Å^2$) 47, HBD 0.8, cLogP 2.8, cLogD (pH 7.4) 2.1 and MW 293. They suggested the following maximum limits when designing compounds as PSA <90 $Å^2$, HBD < 3, cLogP 2-5, cLogD (pH 7.4) 2-5, MW <500. As this was the first round of compound design we restricted the compounds to the following parameters: PSA 40-70 $Å^2$, HBD < 3, cLogP 2-4.5, MW 250-400.

Virtual libraries of all possible compounds that could be constructed from our in-house chemical inventory were constructed, and minimised to ensure that a wide region of chemical space was explored and structures were not biased to one region. Reaction schemes, intermediates and examples of compounds made are described in the supporting information.

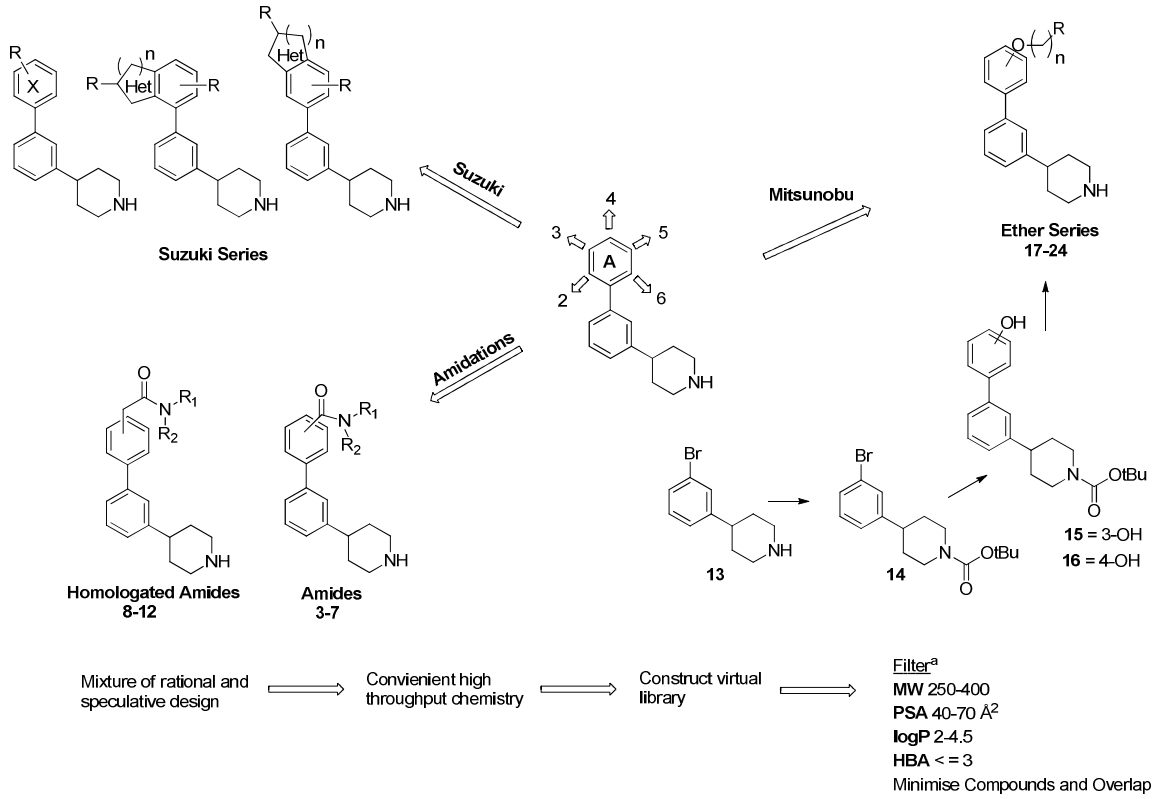

Figure 3. Scaffold Array Chemistry and Design. [a]Filter parameters calculated using the Optibrium STARDROP™ software.

RESULTS AND DISCUSSION

Table 1. Array Chemistry Selected Results for the Amide, Homologated Amides and Ether Series

	Amides	*Tb*NMT IC_{50} (μM)[b]		Homologated Amides	*Tb*NMT IC_{50} (μM)[b]		Ether	*Tb*NMT IC_{50} (μM)[b]
3[a]	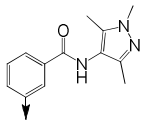	1.7	**8***	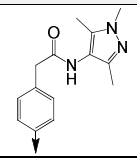	0.4	**17**[a]	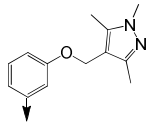	>100
4*	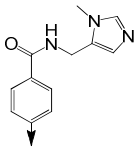	>100	**9***	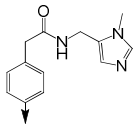	0.60	**18**[a]	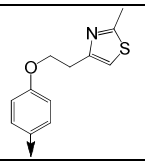	9.5
5[a]	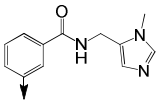	15	**10***	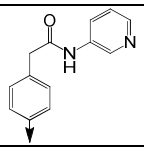	0.07	**19**[a]	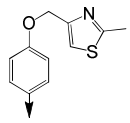	1.6
6[a]	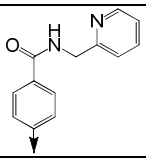	>100	**11***	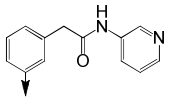	13	**20**[a]	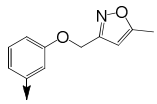	13
7[a]	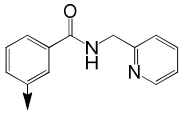	2.9	**12***	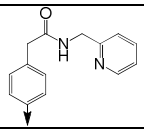	0.60	**21**[a]	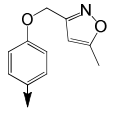	1.4
1[a]	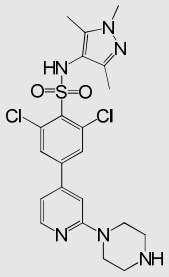	0.002				**22**[a]	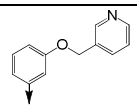	35
						23[a]	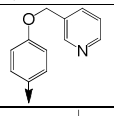	1.2
						24[a]	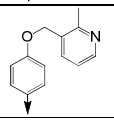	0.5

*Compounds greater than 90% pure, [a]compounds >95% pure

[b]IC_{50} values are shown as mean values of two or more determinations. Standard deviation was typically within 2-fold from the IC_{50}. nd = not determined.

Scaffold array results. No compounds made in the Suzuki chemistry (**1**, Figure 3) derived series had a potency <10 μM against *Tb*NMT, (see supplementary info for compounds made). Table 1 shows the potency against *Tb*NMT for selected examples from the amide (**3-7**), homologated amide (**8-12**) and ether series (**17-24**). The most potent compound in the amide series was **3** (*Tb*NMT IC_{50} 1.7 μM). Amides directly linked to the phenyl ring in the 3-position were found to be more potent than the corresponding 4-substituted analogues (**5** vs. **4** and **7** vs. **6**). The homologated amide series in comparison to the amide series were on the whole >3-fold more potent (**6** vs. **12**) with the most potent compound achieving a *Tb*NMT IC_{50} value of 0.07 μM (**10**). In the homologated amides series the 4-position amides showed greater potency than the corresponding 3-position analogues (the opposite trend to the amide series). Further optimisation of both the directly linked and homologated amide series failed to improve the potency or the pharmacokinetic properties.

The ether array produced compounds with good levels of activity against *Tb*NMT, the most active of these achieved an IC_{50} value 0.5 μM (**24**). The more potent compounds were substituted in the 4-position, on average showing around 10-fold greater potency over their 3-position analogues e.g. 3- compound **22** (35 μM) vs. 4- compound **23** (1.2 μM) or 3- compound **20** (13 μM) vs. 4- compound **21** (1.4 μM). Interestingly, the replacement of the sulfonamide in structure **1** with an ether linkage (**17**) was completely inactive against *Tb*NMT (IC_{50} > 100 μM). This was surprising, as methyl ethers are considered possible sulfonamide bioisosteres[31]. Compound **24** was not selective over human NMT (*Hs*NMT1) but exhibited an EC_{50} of 2 μM in the *T. br. brucei* proliferation assay, with good microsomal stability and moderate levels of selectivity against proliferating human MRC-5 cells (Figure 4).

The crystal structure of **24** bound to *Af*NMT (Figure 4 panel A), shows the ligand binds in the peptide binding groove in an overall U–shaped conformation, with the ligand wrapping round the side chain of Phe157. The central aryl rings of **24** lie perpendicular to each other allowing the ligand to sit in the cleft formed by the side chain of Tyr263, Tyr393 and Leu436. The cleft is formed by the movement of the side chain of Tyr273; a feature observed in binding mode of benzofuran ligands[26-27] and subsequent derivatives[34].

The pyridyl nitrogen of **24** forms an interaction with Ser378 in a similar orientation as the trimethyl-pyrazole group of **1** and the piperidine moiety interacts directly with the C-terminal carboxyl group of Leu492.

Compound **24** does not interact with His265, an interaction formed by the sulfonamide in **1** (overlaid with **24**, Figure 4 panel B), which potentially explained the drop off in potency between **1** (*Tb*NMT 0.002 μM) and (**24**, 0.5μM). Despite this loss of activity, **24** had comparable ligand efficiency (LE)[35] 0.33 to **1** LE 0.36, and in combination with the observed binding mode gave us confidence that the design strategy was valid.

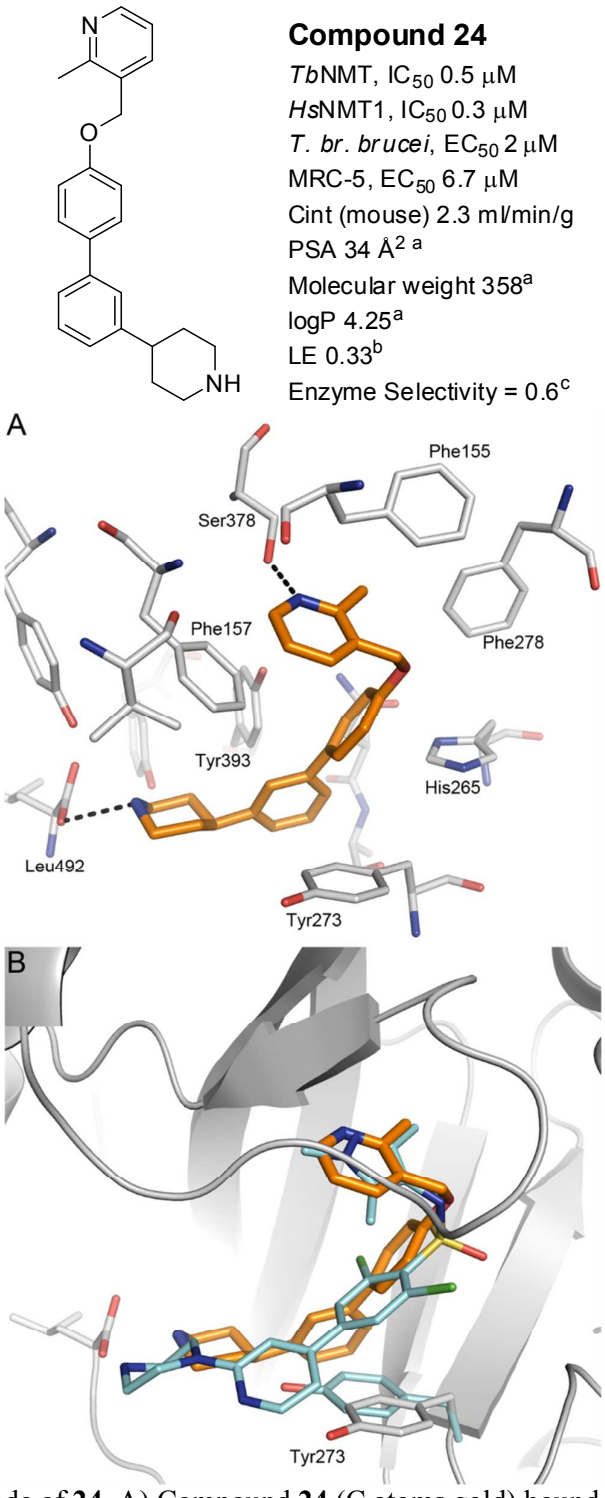

Figure 4. Binding mode of **24**. A) Compound **24** (C atoms gold) bound to *Af*NMT (C atoms grey) PDB 5T5U. H-bonds are shown as dashes lines and key residues labelled. B) A comparison of the binding mode of **24** with **1** bound to *Af*NMT (PDB 4CAX) highlighting the

movement of Tyr273. Compound **1** and the side chain of Tyr273 (4CAX) are shown with cyan C atoms.

Optimization of compound 24. With the aim of increasing potency against *Tb*NMT the diphenyl piperidine ring was replaced with the dichlorophenyl-pyridyl-piperidine moiety of **1**. This change reduced the logP by ~ 1 log unit from 4.3 for **24**, with an increase in PSA from 34 $Å^2$ (19) to 50 $Å^2$ which was within the acceptable guidance limits for BBB permeability[32-33] to give **29** (synthesis shown in Scheme 1).

Compound **29** (Figure 5) exhibited a 4-fold improvement in potency against *Tb*NMT (IC_{50} 0.1 μM), and improved efficacy in the *T. br. brucei* proliferation assay (EC_{50} 0.7 μM), whilst retaining good microsomal stability (1.4 ml/min/g) and LE 0.33. Encouragingly **29** showed good levels of brain penetration (brain:blood, 0.4), a significant improvement over **1** (brain:blood <0.1)[22] indicating that the strategy of reducing MW and PSA was a valid approach (**1**, PSA 101 Å, MW 495). The crystal structure of **29** bound to AfNMT (Figure 6) was determined showing the ligand adopted a conformation similar to **1** with the biaryl system sitting in plane with the 2,6-dichlorophenyl ring stacking in plane with the side chain of Tyr273. Key interactions between the piperidine N to Ser378 and the piperazine to the C-terminal carboxyl group are retained from **24**.

Scheme 1[a]

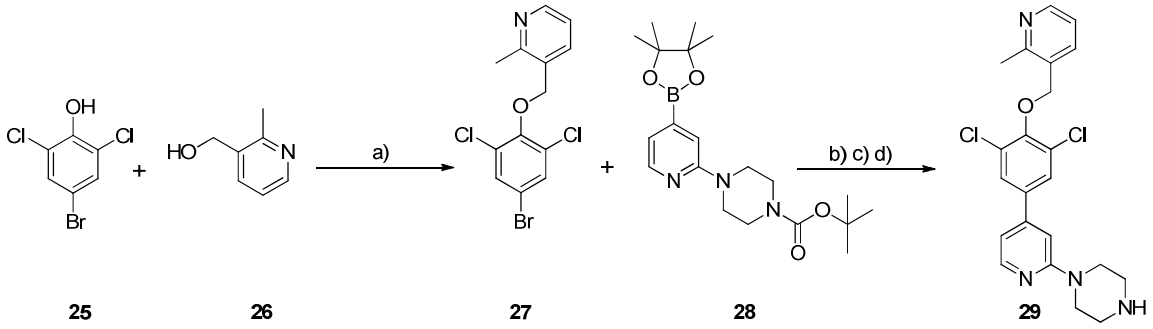

[a]Reagents and conditions: (a) Polymer supported-PPh_3, DIAD, alcohol, THF; (b) dioxane/1 M aq K_3PO_4, $Pd(PPh_3)_4$; (c) TFA, DCM; (d) 2 M HCl in diethyl ether.

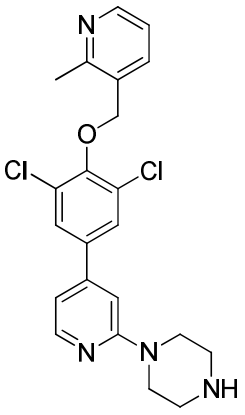

Compound 29

*Tb*NMT, IC_{50} 0.1 μM
*Hs*NMT1, IC_{50} 0.3 μM
T. br. brucei, EC_{50} 0.7 μM
MRC-5, EC_{50} 3.7 μM
Cint (mouse) 1.4 ml/min/g
PSA 50 Å[2a]
Molecular weight 429[a]
logP 3.4[a]
LE 0.33[b]
Enzyme Selectivity = 3[c]

Figure 5. Compound **29** Profile. [a]Values calculated using the Optibrium STARDROP™ software. [b]Ligand efficiency (LE), calculated as 0.6*ln(IC_{50})/(heavy atom count) using *T. brucei* NMT IC_{50} potency[25]. IC_{50} values are shown as mean values of two or more determinations. Standard deviation was typically within 2-fold from the IC_{50}. nd = not determined. [c]Enzyme selectivity calculated as *Hs*NMT1 IC_{50} (μM)/ *Tb*NMT IC_{50} (μM).

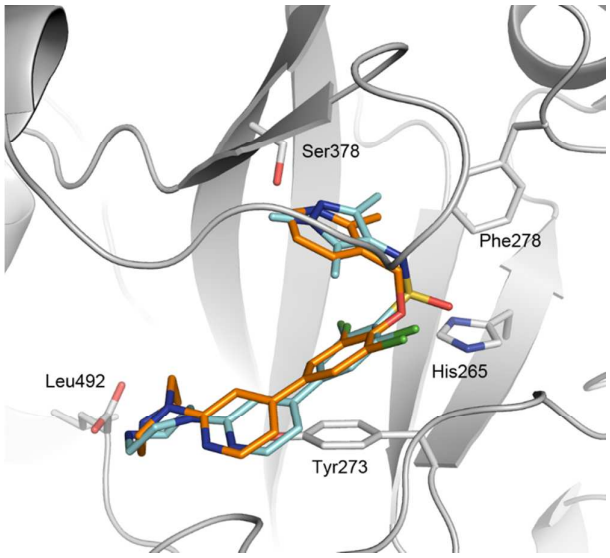

Figure 6. Binding mode of **29** (C atoms gold) bound to *Af*NMT (PDB 5T6C). Binding mode of **1** (C atoms cyan) is shown for comparison.

Replacement of the 2,6-dichlorophenyl ring. Optimisation of **29** focused on modifications to the central 2,6-dichlorophenyl ring to increase enzymatic selectivity relative to *Hs*NMT1 (0.3 μM, 3-fold compared to *Tb*NMT IC_{50}). These modifications were made employing the same chemistry as outlined in Scheme 1, by varying the starting substituted bromophenol used in the Mitsunobu step. These 2,6-dichlorophenyl modifications are detailed in Table 2.

None of the core modifications improved potency against *Tb*NMT when compared to **29** (Table 2) nor LE and enzyme selectivity, although some demonstrated increased levels of potency against *Hs*NMT1 (**37**, *Hs*NMT1, IC_{50} 0.01 μM). The reason for this increase in *Hs*NMT1 activity was not explained using the available crystal structure data. Certainly inhibitors of human NMT such as **37** are of potential interest in the treatment of cancer[20] and further elaboration of the core could be further explored.

Table 2. Modifications to the 2,6-dichorophenyl central ring of compound **29**.

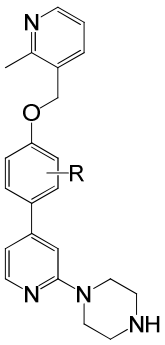

	R	*Tb*NMT IC_{50} (μM)[a]	*Hs*NMT1 IC_{50} (μM)[a]	*T.br. brucei* Tryps EC_{50} (μM)	MRC-5 EC_{50} (μM)	LE[b]	Enzyme Selectivity[c]
29	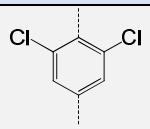	**0.1**	**0.3**	**0.7**	**3.7**	**0.33**	**3**
36	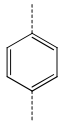	0.6	0.09	2.8	5.0	0.31	0.15
37	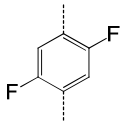	0.8	0.01	2.2	1.5	0.29	0.01
38	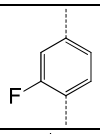	1.2	0.06	2.4	3.3	0.29	0.05
39	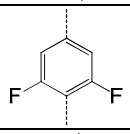	2.0	0.03	2.8	2.5	0.27	0.02
40	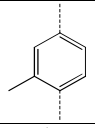	2.0	0.08	2.2	8.7	0.28	0.04
41	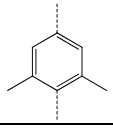	16	1.8	2.7	8.9	0.23	0.11

[a]IC_{50} values are shown as mean values of two or more determinations. Standard deviation was typically within 2-fold from the IC_{50}. nd = not determined. [b]Ligand efficiency (LE), calculated as 0.6*ln(IC_{50})/(heavy atom count) using *T. brucei* NMT IC_{50} potency[25]. [c]Enzyme selectivity calculated as *Hs*NMT1 IC_{50} (μM)/ *Tb*NMT IC_{50} (μM).

Pyridyl head group SAR. The next phase of optimisation focused on modifications to the ether pyridyl ring of **29** shown in Table 3. These compounds were made using the same common phenol intermediate (Scheme 2), applying solid phase reagents such as polystyrene bound triphenylphosphine, and running reactions and purifications in parallel using

commercially available alcohols, or alcohols derived from commercially available carboxylic acids or esters after reduction with borane or lithium aluminium hydride (see supporting information).

Table 3. Pyridyl Head Group SAR of Compound **29**

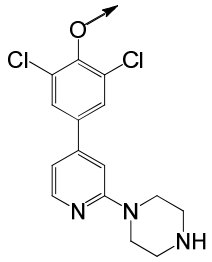

	R	*Tb*NMT IC_{50} (μM)[a]	*Hs*NMT1 IC_{50} (μM)[a]	*T. br. brucei* Tryps EC_{50} (μM)	MRC-5 EC_{50} (μM)	LE[b]	Enzyme Selectivity[c]
29	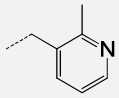	**0.1**	**0.3**	**0.7**	**3.7**	**0.33**	**3**
45	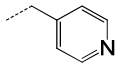	5.4	>1	>25	>1	0.26	nd
46	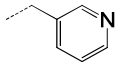	1.6	0.1	>1	>1	0.28	0.67
47	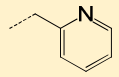	0.1	6.5	0.4	4.6	0.34	65
48	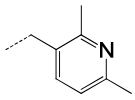	0.8	1.3	0.6	2.8	0.28	1.6
49	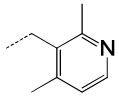	0.3	0.2	0.5	2.3	0.31	0.7
50	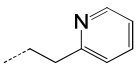	0.8	>1	>1	>1	0.29	nd
51	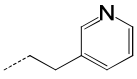	1.3	0.5	>10	>1	0.28	0.4
52	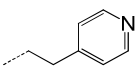	4.6	0.7	>10	>1	0.25	0.15

[a]IC_{50} values are shown as mean values of two or more determinations. Standard deviation was typically within 2-fold from the IC_{50}. Nd = not determined. [b]Ligand efficiency (LE), calculated as 0.6*ln(IC_{50})/(heavy atom count) using *T. brucei* NMT IC_{50} potency[25]. [c]Enzyme selectivity calculated as *Hs*NMT1 IC_{50} (μM)/ *Tb*NMT IC_{50} (μM).

Modifications to the pyridyl head group showed encouraging results with **47** equipotent to **29** (IC_{50} ~ 0.1 μM) but with ~ 65-fold selectivity over *Hs*NMT1, equivalent activity in the *T. br. brucei* proliferation assay, and promising microsomal stability (C_{int} 4.2 ml/min/g). Compound **30** though had equivalent activity to **29** in the MRC-5 counter screen, indicating that *Hs*NMT1 activity may not have been driving the MRC-5 toxicity.

Homologation of the linker to the pyridyl group did not improve potency, as did groups on the pyridyl ring at the 6- (**48**) or 4- (**49**) position though both **48** and **49** showed equivalent activity in the *T. br. brucei* proliferation assay to **29**. The crystal structure of **29** overlaid with the trimethylpyrazole of **1** suggested that additions of methyl substitution may have been beneficial to potency (Figure 7 panel A), because the trimethyl substitution of pyrrole in **1** was essential for activity. Subsequent crystal structures of **48** showed the binding pocket the pyridyl head group accesses is small and that these substituents in the case of **49** forced the ether pyridyl ring to twist in the pocket to avoid steric clashes with its dichlorophenyl ring and for **48** the 4-methyl forces the pyridyl ring out of the pocket. In both cases the direct hydrogen bond from the pyridyl nitrogen to the serine was broken, but **48** still formed an interaction, though this was now water mediated (Figure 7 panel B).

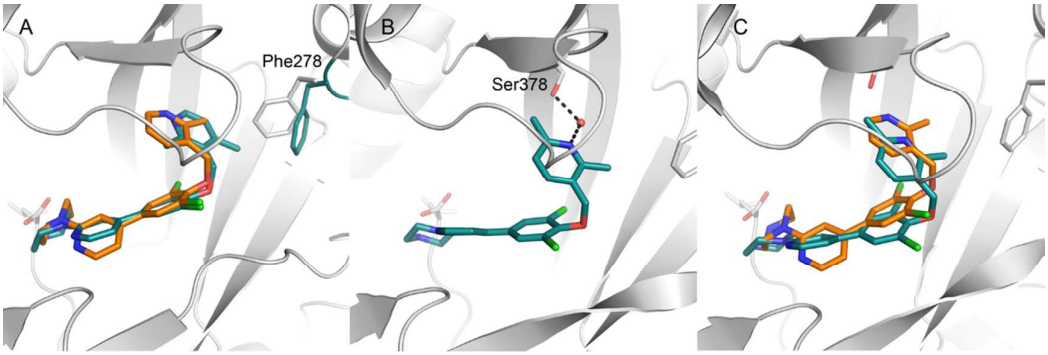

Figure 7. Binding mode of pyridyl head group modifications. Panel A shows binding mode of **49** (C atoms aquamarine) PDB 5T6H compared with **29** (C atoms gold). The side chain of

Phe278 rotates to accommodate the 4-methyl group. Panel B shows the binding mode of **48** (C atoms aquamarine) PDB 5T6E; the interaction with Ser378 is now a water bridged interaction. Panel C shows **48** compared with **29**.

Scheme 2[a]

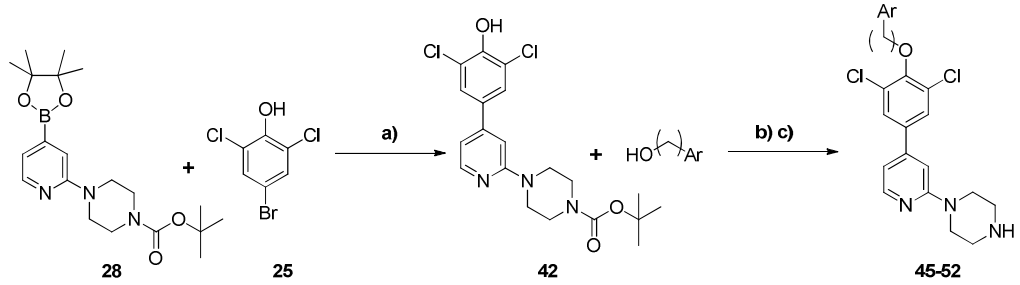

[a]Reagents and conditions: a) Boc_2O, NEt_3, THF; (b) 4-bromo-2,6-dichlorophenol, MeCN/1M aq K_3PO_4, $Pd(dppf)_2Cl_2$, (c) PS-PPh_3, DIAD, alcohol, THF; (d) TFA, DCM.

Alternative non-pyridyl head groups SAR. To advance the series, two regions within the structure were modified with the aim to improve potency, firstly examining pyridyl replacements and modifications to the pyridyl ring and replacement of the piperazino-pyridine moiety. Firstly, the pyridyl ring was replaced with a range of 5-membered heterocycles, mainly thiazoles, with various substitutions, see Table 4. The most potent of these showed levels of promising activity against *Tb*NMT IC_{50} ~ 0.05-0.06 μM (**58** and **57**). The SAR around **57** was tight. The removal of either methyl groups (**60** and **65**) lost activity against *Tb*NMT; in addition substitution of the 2-methyl group with either ethyl (**64**) or isopropyl (**66**) lost all activity in the *T. br. brucei* proliferation assay. Compound **57** showed good stability to microsomal turnover (C_{int} 2.4 ml/min/g) but also improved selectivity over MRC-5 cytotoxicity. Both **58** and **57** showed equivalent levels of potency against *Hs*NMT1 (IC_{50} ~0.03-0.08 μM) and again showed very different MRC-5 activities again indicating that MRC-5 toxicity may not be entirely driven by *Hs*NMT1 activity.

Table 4. Pyridyl Head Group Replacements.

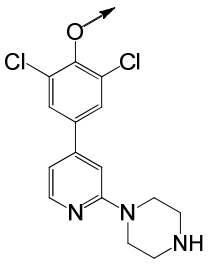

	R	*Tb*NMT IC_{50} (μM)[a]	*Hs*NMT1 IC_{50} (μM)[a]	*T. br. brucei* Tryps EC_{50} (μM)	MRC-5 EC_{50} (μM)	LE[b]	Enzyme Selectivity[c]
29	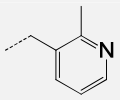	**0.1**	**0.3**	**0.7**	**3.7**	**0.33**	**3**
56	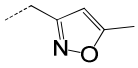	0.3	4.4	1.1	3.5	0.32	15
57	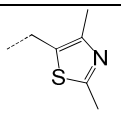	0.05	0.08	0.33	2.2	0.34	2
58	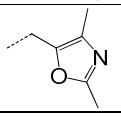	0.06	0.03	0.8	>10	0.34	0.5
59	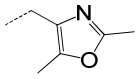	2.9	>100	>100	>100	0.34	>34
60	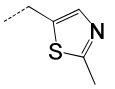	1.3	15	2.8	3.1	0.26	11
61	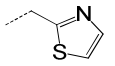	0.3	14	>10	>10	0.29	46
62	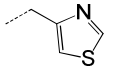	0.5	9.9	>100	>1	0.33	20
63	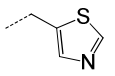	0.2	0.9	>1	>100	0.33	5
64	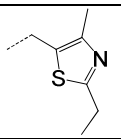	0.3	0.3	>100	>1	0.30	1
65	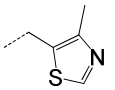	2.0	0.9	>100	>1	0.29	0.5
66	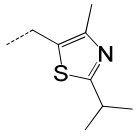	3.5	3.8	>15	2.0	0.24	1

	67	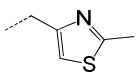	4.2	12	>10	>10	0.24	3

[a]IC_{50} values are shown as mean values of two or more determinations. Standard deviation was typically within 2-fold from the IC_{50}. nd = not determined. [b]Ligand efficiency (LE), calculated as $0.6*\ln(IC_{50})/$(heavy atom count) using *T. brucei* NMT IC_{50} potency[25]. [c]Enzyme selectivity calculated as *Hs*NMT1 IC_{50} (μM)/ *Tb*NMT IC_{50} (μM).

Replacement of the piperazino-pyridine moiety. We had previously validated *Tb*NMT as a druggable target in the stage 2 model for HAT in mice using **68** as a model compound (Figure 8 panel A)[24]. Compound **68** showed good potency in the *T. br. brucei* proliferation assay at EC_{50} 0.001μM and improved levels of selectivity over MRC-5 cells when compared to **1**. We examined hybridising the 4-C chain derivative of **68**, **69**, which showed equally good efficacy and potency and **29** to increase efficacy in the *T. br. brucei* proliferation assay. Compound **71** (synthesis Scheme 3) showed increased selectivity over MRC-5 cells and *Hs*NMT1, but showed a significant drop off in efficacy in the *T. br. brucei* proliferation assay. This was potentially caused by the significant increase in lipophilicity of **71** (logP 5.5) compared to **29** (logP 3.4) resulting in an increase level of non-specific protein/membrane binding. Given the more favourable logP of **29**, further optimization focused on derivatives of **29** rather than **71**. Compound **70** (Scheme 3), the NH piperidine of **71** showed no *in vitro* activity against *Tb*NMT.

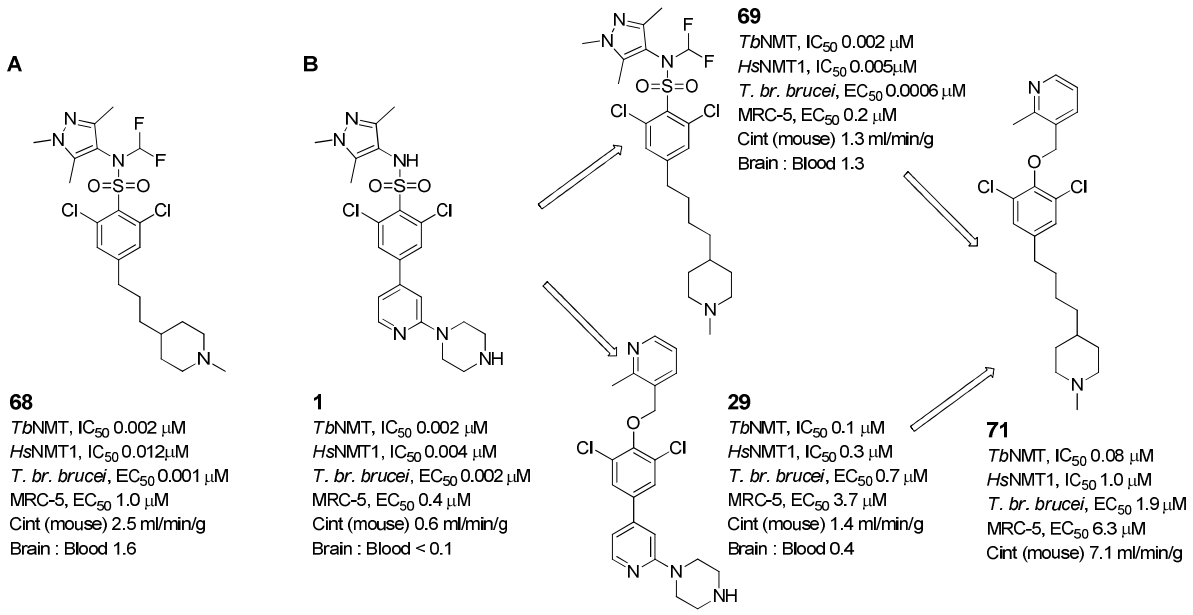

Figure 8. Hybridization Approach

Scheme 3[a]

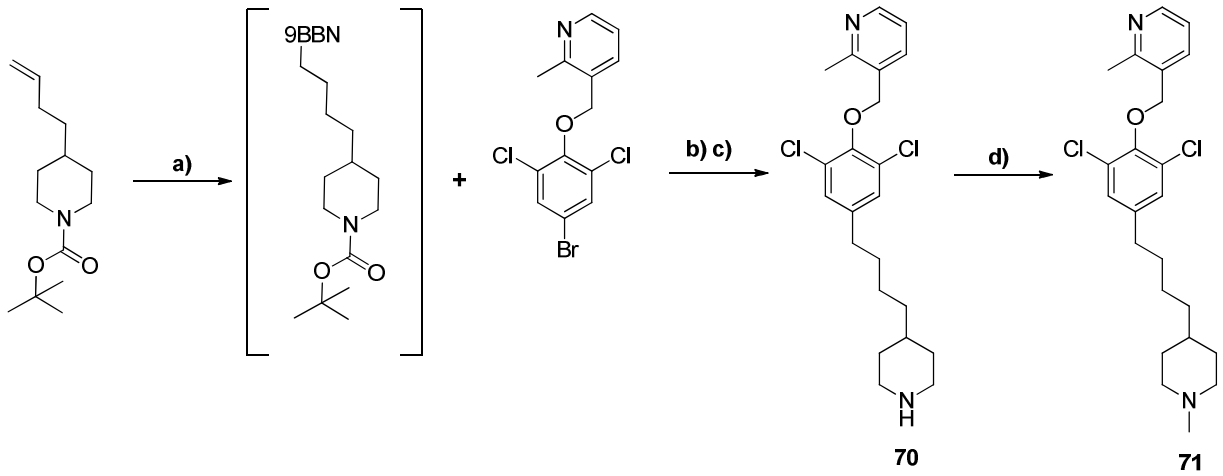

[a]Reagents and conditions: a) 9-BBN, THF; b) $Pd(PPh_3)$,K_3PO_4, H_2O, DMF; c) TFA, DCM; d) CH_2O, $Na(OAc_3)_3BH$, $CHCl_3$.

Pyridyl head group optimisation. The crystal structure of **29** (Figure 6) indicated that the methyl substituent on the pyridyl ring was pointing into a small pocket. Chemistry was developed to explore this pocket with various hydrophobic and polar groups as detailed in

Scheme 4. Using a common intermediate (ethyl 2-chloronicotinate, **72**), Suzuki and Negishi reactions were used to install aromatics rings (**73**) and alkyl groups (**74a-c)** respectively. Amines were installed through displacement of the chlorine of **72**. After reduction of the ethyl esters (**73-75**) to the corresponding alcohols (**76-78**), they were reacted using standard Mitsunobu conditions (Scheme 2) to give final products detailed in Table 5.

Scheme 4[a]

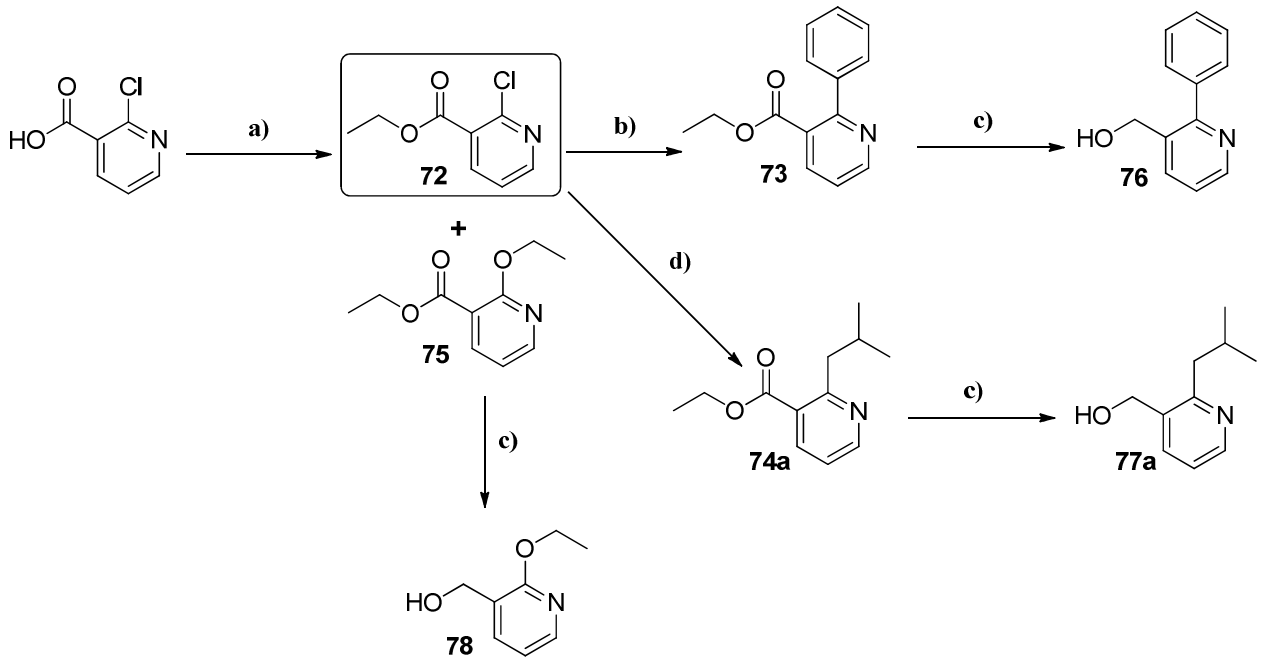

[a]Reagents and conditions: (a) H_2SO_4, EtOH; (b) Phenylboronic acid, 1 M K_3PO_4/dioxane, $Pd(PPh_3)_4$; (c) $LiAlH_4$ 2 M in THF, 0°C; (d) $Pd(^tBuP)_2$, 0.5 M isobutylzinc bromide, anhydrous THF.

Table 5. Pyridyl Substitutions

	R	*Tb*NMT IC_{50} (μM)[a]	*Hs*NMT1 IC_{50} (μM)[a]	*T. br. brucei* EC_{50} (μM)	MRC-5 EC_{50} (μM)	LE[b]	Enzyme Selectivity[c]
	29	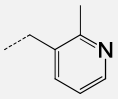	**0.1**	**0.3**	**0.7**	**3.7**	**0.33**	**3**
	79	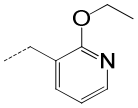	>50	>50	>50	>50		
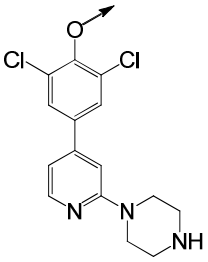	**80**	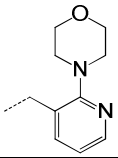	0.1	0.04	>10	14	0.28	0.4
	81	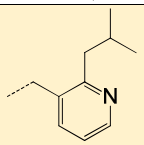	**0.02**	**0.04**	**0.1**	**1.5**	**0.33**	**2**
	82	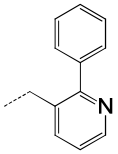	0.08	0.2	0.1	2.1	0.28	3
	83	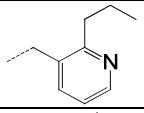	0.02	0.04	0.3	>1	0.34	2
	84	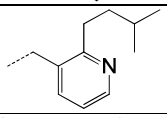	0.06	0.18	0.5	1.4	0.29	3

[a]IC_{50} values are shown as mean values of two or more determinations. Standard deviation was typically within 2-fold from the IC_{50}. nd = not determined. [b]Ligand efficiency (LE), calculated as 0.6*ln(IC_{50})/(heavy atom count) using *T. brucei* NMT IC_{50} potency[25]. [c]Enzyme selectivity calculated as *Hs*NMT1 IC_{50} (μM)/ *Tb*NMT IC_{50} (μM).

Good levels of inhibition of *Tb*NMT were observed for all compounds prepared (except **79**), some with improved potency over **29**. The loss of activity of **79** was most probably caused by the alkoxy-group reducing the basicity of the pyridine ring, making the ring nitrogen a poorer HBA. Compounds **81** and **82** showed promising potency against the parasite (EC_{50} = 0.1 μM) with good selectivity compared to MRC-5 cells (**81**) and had good microsomal stability (**81** 1.2 ml/min/mg, **82** 1.6 ml/min/mg). Compound **81** (Figure 9)

showed significant levels of brain penetration (brain:blood ratio 1.9), a significant improvement on **29** (brain:blood ratio 0.4), and **1** (brain:blood ratio <0.1). Compound **81** represents a good lead for further optimization to identify candidates for development for stage 2 HAT.

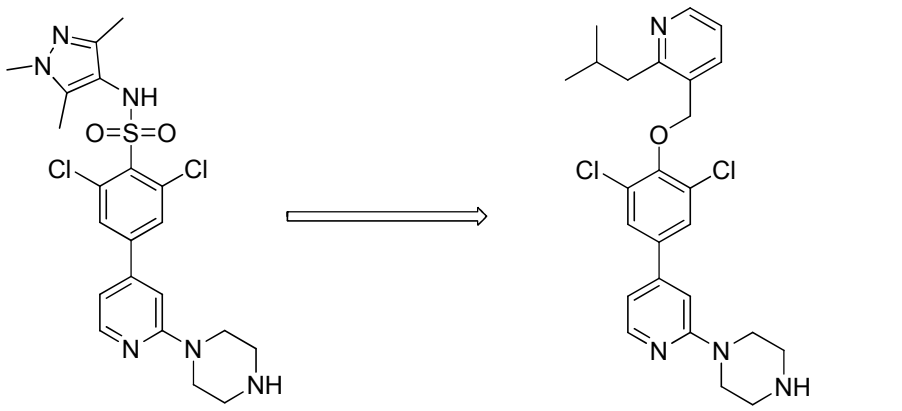

1: DDD85646
*Tb*NMT, IC_{50} 0.002 μM
*Hs*NMT1, IC_{50} 0.004 μM
T. br. brucei, EC_{50} 0.002 μM
MRC-5, EC_{50} 0.4 μM
Cint (mouse) 0.6 ml/min/g
Brain : Blood < 0.1
PSA 101 $Å^2$
Molecular weight 495
logP 3.1
LE 0.36
Enzyme Selectivity = 2

81
*Tb*NMT, IC_{50} 0.02 μM
*Hs*NMT1, IC_{50} 0.04 μM
T. br brucei, EC_{50} 0.12 μM
MRC-5, EC_{50} 1.5 μM
Cint (mouse) 1.2 ml/min/g
Brain : Blood 1.9
PSA 50 $Å^2$
Molecular weight 471
logP 4.2
LE 0.33
Enzyme Selectivity = 2

Figure 9. Comparison of **1** and **81**

CONCLUSIONS

Using **1** as a start point to identify alternative *Tb*NMT inhibitor scaffolds with physicochemical properties suitable for penetration into the brain to treat stage 2 HAT, we identified an ether linker as a replacement of the sulfonamide of **1**. This modification reduced molecular weight and polar surface area, producing a viable alternative series with excellent levels of brain penetration. This work highlights the importance of decreasing the PSA as a way of increasing the probability of brain penetration. Further optimization identified compounds with good levels of *Tb*NMT and *T. br. brucei* anti-proliferative activity, and microsomal stability. Though in comparison with the original structure **1**, further potency gains against the enzyme and in the parasite proliferation assay are required. This series presents good leads to identify potential development candidates for stage 2 HAT.

Experimental Section

Synthetic Materials and Methods. Chemicals and solvents were purchased from the Aldrich Chemical Company, Fluka, ABCR, VWR, Acros, Fisher Chemicals and Alfa Aesar and were used as received unless otherwise stated. Air- and moisture-sensitive reactions were carried out under an inert atmosphere of argon in oven-dried glassware. Analytical thin-layer chromatography (TLC) was performed on pre-coated TLC plates (layer 0.20 mm silica gel 60 with fluorescent indicator UV254, from Merck). Developed plates were air-dried and analyzed under a UV lamp (UV254/365 nm). Flash column chromatography was performed using pre-packed silica gel cartridges (230-400 mesh, 40–63 μm, from SiliCycle) using a Teledyne Presearch ISCO Combiflash Companion 4X, or Combiflash Retrieve. ^{1}H NMR and ^{13}C NMR spectra were recorded on a Bruker Avance II 500 spectrometer (^{1}H at 500.1 MHz, ^{13}C at 125.8 MHz) or a Bruker DPX300 spectrometer (^{1}H at 300.1 MHz). Chemical shifts (δ) are expressed in ppm recorded using the residual solvent as the internal reference in all cases.

Signal splitting patterns are described as singlet (s), doublet (d), triplet (t), quartet (q), pentet (p), multiplet (m), broad (br), or a combination thereof. Coupling constants (*J*) are quoted to the nearest 0.1 Hz. LC-MS analyses were performed with either an Agilent HPLC 1100 series connected to a Bruker Daltonics micrOTOF, or an Agilent Technologies 1200 series HPLC connected to an Agilent Technologies 6130 quadrupole LC-MS, where both instruments were connected to an Agilent diode array detector. LC-MS chromatographic separations were conducted with a Waters Xbridge C18 column, 50 mm x 2.1 mm, 3.5 μm particle size; mobile phase, water/acetonitrile +0.1% HCOOH, or water/acetonitrile + 0.1% NH_3; linear gradient 80:20 to 5:95 over 3.5 min, and then held for 1.5 min; flow rate 0.5 mL min^{-1}. All assay compounds had a measured purity of ≥95% (by TIC and UV) as determined using this analytical LC-MS system, a lower purity level is indicated. High resolution electrospray measurements were performed on a Bruker Daltonics MicrOTOF mass spectrometer. Microwave-assisted chemistry was performed using a Biotage Initiator Microwave Synthesizer.

*tert-Butyl-4-(3-bromophenyl)piperidine-1-carboxylate (**14**)*. A solution of 4-(3-bromophenyl)piperidine.hydrochloride (**13**) (5.1 g, 18.4 mmol, 1 eq), Boc_2O (4.4 g, 20.2 mmol, 1.1eq), and triethylamine (3.87 mL, 27.8 mmol, 1.5 eq) in THF (50 mL) was stirred at room temperature for 16 h. The reaction was filtered, the filtrate washed with dilute 10% citric acid and extracted into ethyl acetate. The ethyl acetate layer was washed with water, then dried over $MgSO_4$, filtered and evaporated to give an off-white solid (**14**) (6.13 g, 98% yield). ^{1}H NMR, 500MHz, $CDCl_3$ δ1.51 (s, 9H), 1.57-1.66 (m, 2H), 1.81-1.86 (m, 2H), 2.64 (tt, *J* = 3.70, 12.21, 1H), 2.77-2.85 (m, 2H), 4.22-4.32 (m, 2H), 7.14-7.22 (m, 2H), 7.35-7.39 (m, 2H). $[M+H]^+$ = 388.4

*tert-Butyl 4-(3'-hydroxy-[1,1'-biphenyl]-3-yl)piperidine-1-carboxylate (**15**)*. tert-Butyl 4-(3-bromophenyl)piperidine-1-carboxylate (**14**) (2 g, 5.88 mmol, 1 eq), 3-hydroxyphenyl boronic

acid (974 mg 7.06 mmol, 1.2 eq), anhydrous dioxane (10 mL) and 1 M aq K_3PO_4 (6 mL) were combined in a microwave vessel and argon bubbled through the mixture for 5 min. $Pd(PPh_3)_4$ (136 mg, 0.118 mmol, 2%), was added and the reaction degassed again for a further 5 min before microwaving at 140 ^oC for 15 min. The resulting solution was extracted into dichloromethane, washed with sat. aq. $NaHCO_3$, and passed through a phase separation cartridge, the organic layer was then absorbed onto silica and purified by flash column chromatography running a gradient from 0% ethyl acetate/hexane to 50% ethyl acetate/hexane, to give **15** as a colourless oil (1.76 g, 85% yield). ^1H NMR 500MHz, $CDCl_3$ δ 1.53 (s, 9H), 1.60-1.76 (m, 2H), 1.83-1.91 (m, 2H), 2.71 (tt, *J* = 3.68, 12.33, 1H), 2.70-2.91 (m, 2H), 4.24-4.35 (m, 2H), 6.36 (s, 1H), 6.88 (dd, *J* = 2.50, 8.11, 1H), 7.10-7.20 (m, 3H), 7.28-7.46 (m, 4H).

*tert-Butyl 4-(4'-hydroxy-[1,1'-biphenyl]-3-yl)piperidine-1-carboxylate (**16**).* Made using 4-hydroxyphenylboronic acid (183 mg, 1.32 mmol, 1 eq), tert-butyl 4-(3-bromophenyl)piperidine-1-carboxylate (**14**) (450 mg, 1.32 mmol, 1 eq), $Pd(PPh_3)_4$ (30 mg) and K_3PO_4 (1 eq) in DMF:H_2O (3:1, 4 ml) to afford **16** (326 mg, 70% yield). ^1H NMR 500MHz, DMSO, δ 1.56 (s, 9H), 1.68-1.74 (m, 2H), 1.86-1.96 (m, 2H), 2.72-2.80 (m, 1H), 2.80-3.00 (m, 2H), 4.29-4.32 (br. s, 2H), 5.02 (s, 1H), 6.96-6.99 (m, 2H), 7.18-7.21 (m, 1H), 7.39-7.48 (m, 3H), 7.52-7.56 (m, 2H). $[M+H]^+$ = 354.2331, 298.1651 (product – ^{t}Bu)

*4-(3'-((1,3,5-Trimethyl-1H-pyrazol-4-yl)methoxy)-[1,1'-biphenyl]-3-yl)piperidine (**17**).* tert-Butyl 4-(3'-hydroxy-[1,1'-biphenyl]-3-yl)piperidine-1-carboxylate (**15**) (100 mg, 0.28 mmol, 1 eq), (1,3,5-trimethylpyrazole)methanol (44 mg, 0.31 mmol, 1.1 eq), polystyrene bound-PPh_3 (PPh_3 = triphenylphosphine, 1.84 mmol/g loading, 228 mg, 0.42 mmol, 1.5 eq), diisopropyl azodicarboxylate (DIAD, 66 uL, 0.34 mmol, 1.2 eq) in anhydrous dioxane (5 mL) in a capped test tube was heated at 60 ^oC for 16 h. The reaction was absorbed onto silica and purified by flash column chromatography running a gradient from 0% ethyl

acetate/hexane to 100% ethyl acetate. The resulting product was evaporated *in vacuo* before dissolving in dichloromethane (10 mL), addition of trifluoroacetic acid (10 eq) and stirring at RT for 3 h. The reaction was then evaporated *in vacuo* before dissolving in dichloromethane and loading onto a pre-washed SCX cartridge. The SCX cartridge was washed with dichloromethane (3 x 10 mL) and MeOH (3 x 10 mL) before eluting the product with 7 N ammonia in methanol. This was evaporated to give **17** (64 mg, 61% yield). ^{1}H NMR 500MHz, $CDCl_3$ δ 1.66 (s, 3H), 1.67-1.75 (m, 2H), 1.87-1.92 (m, 2H), 2.70-2.77 (m, 1H), 2.80-2.89 (m, 2H), 3.76 (s, 3H), 4.22-4.35 (m, 2H), 4.90 (s, 2H), 6.39 (br. s, 1H), 6.98-7.01 (m, 1H), 7.20-7.23 (m, 3H), 7.37-7.47 (m, 4H). [M+H] = 427.2.

Compounds **14-20** were made in an analogue manner to **17** from **16**, see Supporting Information for analytical data.

Prototypical Mitsunobu reaction of a pyridyl alcohol and a substituted phenol (Scheme 1)

(See Supporting Information *for the synthesis of intermediates 30-35 for compounds 36-41, Table 2).*

*3-((4-Bromo-2,6-dichlorophenoxy)methyl)-2-methylpyridine (**27**).* DIAD (diisopropyl azodicarboxylate, 5 mL, 24.8 mmol, 1.2 eq) was added to a suspension of 4-bromo-2,6-dichlorophenol (**25**) (5.0 g, 20.7 mmol, 1 eq) and 2-methyl-3-hydroxymethylpyridine (**26**) (3.1 g, 24.8 mmol, 1.2 eq), polystyrene bound-PPh_3 (1.84 mmol/g loading, 16.2 g, 29.8 mmol, 1.2 eq), in anhydrous THF (20 mL) then heated at 70 ^{o}C for 4 h. After cooling the reaction mixture was filtered, the beads washed with MeOH and dichloromethane, and the filtrate concentrated *in vacuo*. The resulting residue was triturated with MeOH to give **27** as a white solid (5.46 g, 76% yield). ^{1}H NMR 500MHz, $CDCl_3$ δ 2.68 (s, 3H), 5.03 (s, 2H), 7.18 (dd, J = 4.90, 7.68Hz, 1H), 7.49 (s, 3H), 7.82 (dd, J = 1.68, 7.68Hz, 1H), 8.50 (dd, J = 1.68, 4.90Hz, 1H). LCMS $[M+H]^+$ = 347.9.

*tert-Butyl 4-(4-(4,4,5,5-tetramethyl-1,3,2-dioxaborolan-2-yl)pyridin-2-yl)piperazine-1-carboxylate (**28**).* A solution of 1-(4-(4,4,5,5-tetramethyl-1,3,2-dioxaborolan-2-yl)pyridin-2-yl)piperazine (2.97 g, 10.27 mmol, 1 eq), di-tert-butyl-dicarbonate (Boc_2O, 2.5 g, 11.3 mmol, 1.1 eq), in THF (20 mL) and triethylamine (2.1 mL, 15.4 mmol, 1.5 eq) was stirred at RT overnight. The resulting reaction was extracted into dichloromethane, and then washed with 10% citric acid and then water. The dichloromethane layer was dried over $MgSO_4$, filtered and evaporated to give (**28**) as a white solid (4 g, 100% yield). ^{1}H NMR 500MHz, $CDCl_3$ δ 1.28 (s, 12H), 1.42 (s, 9H), 3.45-3.50 (m, 8H), 6.90 (d, J = 4.91, 1H), 6.97 (s, 1H), 8.14 (dd, J = 1.02, 4.89, 1H). $[M+H]^+$ = 389.45

Prototypical Suzuki reaction of an aryl bromide and a boronate ester (Compounds 29-35).

*1-(4-(3,5-Dichloro-4-((2-methylpyridin-3-yl)methoxy)phenyl)pyridin-2-yl)piperazine dihydrochloride salt (**29**).*tert-Butyl 4-(4-(4,4,5,5-tetramethyl-1,3,2-dioxaborolan-2-yl)pyridin-2-yl)piperazine-1-carboxylate (**28**) (67 mg, 0.23 mmol, 1eq), 3-((4-bromo-2,6-dichlorophenoxy)methyl)-2-methylpyridine (**27**) (80 mg, 0.23 mmol, 1eq), and potassium phosphate.trihydrate (49 mg, 0.231 mmol, 1 eq) in DMF:H_2O (1:1, 4 mL) was combined in a microwave vessel and degassed with argon for 5 min, before the addition of $Pd(PPh_3)_4$ (14 mg, 0.012 mmol, 5%), and reaction degassed again, then microwaved at 100 ^{o}C for 40 min. Reaction was concentrated *in vacuo*, extracted into dichloromethane and then washed with aq. $NaHCO_3$. The two phase system was passed through a phase separation cartridge, the filtrate concentrated *in vacuo* and the title compound purified by flash column chromatography using 8% MeOH/ethyl acetate + 1% aq NH_3 as the eluent. The residue was taken up in dichloromethane, ethereal HCl was added (2 M, 2 mL), concentrated and the di-hydrochloride salt of **29** triturated with ether, filtered and washed with ether. (104 mg, 71% yield). ^{1}H NMR 500MHz, *d6*-DMSO δ 2.82 (s, 3H), 3.17-3.23 (m, 4H), 3.85-3.90 (m, 4H), 5.29 (s, 2H), 7.16 (d, J = 5.20Hz, 1H), 7.27-7.30 (m, 1H), 7.78-7.86 (m, 1H), 8.06 (s, 2H),

8.22 (d, *J* = 5.20Hz, 1H), 8.41-8.51 (m, 1H), 8.71-8.77 (m, 1H), 9.15 (br s, 2H). HRMS $[M+H]^+$ calculated for $C_{22}H_{23}Cl_2N_4O_1$ = 429.1243, found = 429.1240.

*1-(4-(4-((2-Methylpyridin-3-yl)methoxy)phenyl)pyridin-2-yl)piperazine dihydrochloride salt (**36**).* Prepared from 3-((4-bromophenoxy)methyl)-2-methylpyridine (**30**) (150mg, 0.54mmol, 1eq) and 1-(4-(4,4,5,5-tetramethyl-1,3,2-dioxaborolan-2-yl)pyridin-2-yl)piperazine **28** (156mg, 0.54mmol, 1eq), according to the method outlined for the synthesis of **29** to give **36** as a dihydrochloride salt (150mg, 64% yield). ^{1}H NMR 500MHz, DMSO δ 2.79 (s, 2H), 3.21-3.27 (m, 4H), 3.93-3.98 (m, 4H), 5.40 (s, 2H), 7.21-7.30 (m, 3H), 7.35-7.43 (m, 1H), 7.86-7.95 (m, 3H), 8.15 (d, *J* = 6.00Hz, 1H), 8.53 (d, *J* = 7.45Hz, 1H), 8.74 (d, *J* = 5.75Hz, 1H), 9.39 (br s, 2H). LCMS $[M+H]^+$ = 361.2. HRMS $[M+H]^+$ calculated for $C_{22}H_{25}N_4O_1$ = 361.2023, found = 361.2033

*1-(4-(2,5-Difluoro-4-((2-methylpyridin-3-yl)methoxy)phenyl)pyridin-2-yl)piperazine dihydrochloride (**37**).* Prepared from 3-((4-bromo-2,5-difluorophenoxy)methyl)-2-methylpyridine **(31)** (106 mg, 0.34 mmol, 1 eq) and **28** (98 mg, 0.34 mmol, 1eq), according to the method outlined for the synthesis of **29** to give **37** as a dihydrochloride salt (124mg, 78% yield). ^{1}H NMR 500MHz, DMSO δ 2.79 (s, 3H), 3.17-3.23 (m, 4H), 3.84-3.90 (m, 4H), 5.48 (s, 2H), 6.99-7.03 (m, 1H), 7.14-7.19 (m, 1H), 7.57 (dd, *J* = 7.20, 12.20Hz, 1H), 7.75 (dd, *J* = 7.33, 11.83Hz, 1H), 7.90 (t, *J* = 7.90Hz, 1H), 8.20 (d, *J* = 5.55Hz, 1H), 8.49 (d, *J* = 7.25Hz, 1H), 8.76 (d, *J* = 5.65Hz, 1H), 9.32 (br s, 2H). LCMS $[M+H]^+$ = 397.2. HRMS $[M+H]^+$ calculated for $C_{22}H_{23}F_2N_4O_1$ = 397.1834, found = 397.1848

*1-(4-(2-Fluoro-4-((2-methylpyridin-3-yl)methoxy)phenyl)pyridin-2-yl)piperazine dihydrochloride (**38**).* Prepared from 3-((4-bromo-3-fluorophenoxy)methyl)-2-methylpyridine **(32)** (100 mg, 0.34 mmol, 1 eq) and **28** (98 mg, 0.34 mmol, 1 eq), according to the method outlined for the synthesis of **29** to give **38** as a dihydrochloride salt (110 mg, 72% yield). ^{1}H NMR 500MHz, DMSO δ 2.81 (s, 3H), 3.19-3.25 (m, 4H), 3.89-3.96 (m, 4H), 5.42 (s, 2H),

7.02-7.08 (m, 1H), 7.13 (dd, *J* = 1.85, 8.35Hz, 1H), 7.25 (dd, *J* = 1.63, 12.88Hz, 1H), 7.70 (t, *J* = 8.65Hz, 1H), 7.92 (t, *J* = 6.48Hz, 1H), 8.17 (d, *J* = 5.65Hz, 1H), 8.55 (d, *J* = 7.65Hz, 1H), 8.75 (d, *J* = 5.05Hz, 1H), 9.47 (br s, 2H). LCMS $[M+H]^+$ = 379.2. HRMS $[M+H]^+$ calculated for $C_{22}H_{24}F_1N_4O_1$ = 379.1929, found = 379.1942

*1-(4-(2,6-Difluoro-4-((2-methylpyridin-3-yl)methoxy)phenyl)pyridin-2-yl)piperazine dihydrochloride (**39**).* Prepared from 3-((4-bromo-3,5-difluorophenoxy)methyl)-2-methylpyridine (**33**) (106 mg, 0.34 mmol, 1 eq) and **28** (98 mg, 0.34 mmol, 1 eq), according to the method outlined for the synthesis of **29** to give **39** as a dihydrochloride salt (109 mg, 69% yield). ^{1}H NMR 500MHz, DMSO δ 2.77 (s, 3H), 3.16-3.21 (m, 4H), 3.77-3.82 (m, 4H), 5.40 (s, 2H), 6.82 (d, *J* = 4.95Hz, 1H), 7.03-7.07 (m, 1H), 7.14 (d, *J* = 9.90Hz, 2H), 7.86-7.91 (m, 1H), 8.23 (d, *J* = 5.20Hz, 1H), 8.49 (d, *J* = 6.30Hz, 1H), 8.75 (d, *J* = 5.45Hz, 1H), 9.20 (br s, 2H). LCMS $[M+H]^+$ = 397.2. HRMS $[M+H]^+$ calculated for $C_{22}H_{23}F_2N_4O_1$ = 397.1834, found = 397.1852

*1-(4-(2-Methyl-4-((2-methylpyridin-3-yl)methoxy)phenyl)pyridin-2-yl)piperazine dihydrochloride (**40**).*Prepared from 3-((4-bromo-3-methylphenoxy)methyl)-2-methylpyridine (**34**) (150 mg, 0.51 mmol, 1 eq) and **28** (148 mg, 0.51 mmol, 1 eq), according to the method outlined for the synthesis of **29** to give **40** as a dihydrochloride salt (110 mg, 48% yield). ^{1}H NMR 500MHz, DMSO δ 2.29 (s, 3H), 2.77 (s, 3H), 3.17-3.23 (m, 4H), 3.83-3.88 (m, 4H), 5.34 (s, 2H), 6.80-6.84 (m, 1H), 6.96-7.00 (m, 1H), 7.04 (dd, *J* = 2.58, 8.43Hz, 1H), 7.10 (d, *J* = 2.50Hz, 1H), 7.25 (d, *J* = 8.45Hz, 1H), 7.85 (t, *J* = 6.63Hz, 1H), 8.15 (d, *J* = 5.80Hz, 1H), 8.47 (d, *J* = 7.25Hz, 1H), 8.72 (d, *J* = 5.20Hz, 1H), 9.27 (br s, 2H). LCMS $[M+H]^+$ = 375.2. HRMS $[M+H]^+$ calculated for $C_{23}H_{27}N_4O_1$ = 375.2179, found = 375.2191

*1-(4-(2,6-Dimethyl-4-((2-methylpyridin-3-yl)methoxy)phenyl)pyridin-2-yl)piperazine dihydrochloride (**41**).*Prepared from 3-((4-bromo-3,5-dimethylphenoxy)methyl)-2-methylpyridine **(35**) (150 mg, 0.49 mmol, 1 eq) and **28** (142 mg, 0.49 mmol, 1 eq), according

to the method outlined for the synthesis of **29** to give **41** as a dihydrochloride salt (177 mg, 75% yield). ^{1}H NMR 500MHz, DMSO δ 2.033 (s, 6H), 2.79 (s, 3H), 3.17-3.23 (m, 4H), 3.84-3.89 (m, 4H), 5.31 (s, 2H), 6.63-6.67 (m, 1H), 6.89-6.93 (m, 3H), 7.89 (t, J=6.70Hz, 1H), 8.18 (d, J=5.35Hz, 1H), 8.51 (d, J=7.70Hz, 1H), 8.73 (dd, J=1.10, 5.65Hz, 1H), 9.36 (br s, 2H). LCMS $[M+H]^+$ = 389.2. HRMS $[M+H]^+$ calculated for $C_{24}H_{29}N_4O_1$ = 389.2336, found = 389.235

*tert-Butyl 4-(4-(3,5-dichloro-4-hydroxyphenyl)pyridin-2-yl)piperazine-1-carboxylate (**42**)*. A solution of a tert-butyl 4-(4-(4,4,5,5-tetramethyl-1,3,2-dioxaborolan-2-yl)pyridin-2-yl)piperazine-1-carboxylate **28** (2.0 g, 5.14 mmol, 1.2 eq), and 4-bromo-2,6-dichlorophenol (**25**) (1.04 g, 4.3 mmol, 1 eq) in acetonitrile (7 mL) and aq. 1M K_3PO_4 (5 mL) was degassed by bubbling argon through for 5 min, then $Pd(dppf)_2Cl_2$ (175 mg, 0.22 mmol, 5%) added and the reaction degassed again for a further 5 min before microwaving at 100 ^{o}C for 30 min. The cooled solution was diluted with dichloromethane and washed with aq. $NaHCO_3$, the dichloromethane layer dried over $MgSO_4$, the filtrate evaporated onto silica and purified by flash column chromatography running a gradient from 0% ethyl acetate/hexane to 50% ethyl acetate/hexane to give **42** as a white solid (1.07 g, 49% yield). ^{1}H NMR 500MHz, $CDCl_3$ δ 1.52 (s, 9H), 3.58-3.64 (m, 8H), 6.05 (br. s, 1H), 6.72 (s, 1H), 6.79 (d, *J* = 5.30, 1H), 7.53 (s, 2H), 8.25 (d, *J* = 5.19, 1H). [M+H] = 424.2.

*1-(4-(3,5-Dichloro-4-(2-(pyridin-3-yl)ethoxy)phenyl)pyridin-2-yl)piperazine (**51**).* DIAD (diisopropyl azodicarboxylate, 61 uL, 0.31 mmol, 1.1 eq) was added to a suspension of 2-(pyridin-3-yl)ethanol (42 mg, 0.34 mmol, 1.2 eq), polystyrene bound – PPh_3 (1.84 mmol/g loading, 200 mg, 0.37 mmol, 1.2 eq), and **42** (120 mg, 0.28 mmol, 1 eq) in anhydrous THF (20 mL) and then heated at 70 ^{o}C for 4 h. After cooling the reaction mixture was filtered, the beads washed with MeOH and dichloromethane, the filtrate absorbed onto silica and purified by flash column chromatography running a gradient from 0% ethyl acetate/hexane to 100%

ethyl acetate. The resulting residue was dissolved in dichloromethane (10 mL), trifluoroacetic acid (10 eq) added and the reaction stirred at RT for 16 h. Reaction was evaporated *in vacuo* before loading onto a pre-washed SCX cartridge. The cartridge was washed with dichloromethane (3 x 10 mL) and MeOH (3 x 10 mL) before eluting with 7 N ammonia in methanol. This was absorbed onto silica and purified by flash column chromatography running a gradient from 0% MeOH/dichloromethane + 1% NH_3 to 20% MeOH/dichloromethane + 1% NH_3 to give **51** as a white solid (35 mg, 29% yield). ^{1}H NMR 500MHz, $CDCl_3$ δ 3.02-3.05 (m, 4H), 3.22 (t, *J* = 6.90 Hz, 2H), 3.58-3.61 (m, 4H), 4.30 (t, *J* = 6.90 Hz, 2H), 6.71 (s, 1H), 6.75 (dd, *J* = 1.50, 5.25 Hz, 1H), 7.28-7.31 (m, 1H), 7.52 (s, 2H), 7.72-7.74 (m, 1H), 8.25 (dd, *J* = 0.61, 5.24 Hz, 1H), 8.54 (dd, *J* = 1.61, 4.97 Hz, 1H), 8.63 (d, *J* = 2.11 Hz, 1H). $[M+H]^+$ = 429.1. HRMS $[M+H]^+$ calculated for $C_{22}H_{23}Cl_2N_4O_1$ = 429.1243, found = 429.1245.

*1-(4-(3,5-Dichloro-4-(pyridin-4-ylmethoxy)phenyl)pyridin-2-yl)piperazine (**45**).* Prepared using **42** (120 mg, 0.28 mmol, 1 eq), and pyridin-4-ylmethanol (37 mg, 0.34 mmol, 1.2 eq), according to the Mitsunobu reaction and BOC deprotection procedure outlined for the synthesis **51** to give **45** as an off-white solid (1 mg, 1% yield). ^{1}H NMR 500MHz, $CDCl_3$ δ 3.04-3.06 (m, 4H), 3.61-3.63 (m, 4H), 5.14 (s, 2H), 6.74 (s, 1H), 6.78 (dd, *J* = 1.52, 5.39 Hz, 1H), 7.52-7.53 (m, 2H), 7.58 (s, 2H), 8.28 (d, *J* = 5.25 Hz, 1H), 8.69 (dd, *J* = 1.80, 5.94 Hz, 2H). $[M+H]^+$ = 415.1

*1-(4-(3,5-Dichloro-4-(pyridin-3-ylmethoxy)phenyl)pyridin-2-yl)piperazine (**46**).* Prepared using **42** (120 mg, 0.28 mmol, 1 eq), and pyridin-3-ylmethanol (33 µL, 0.34 mmol, 1.2 eq), according to the Mitsunobu reaction and BOC deprotection procedure outlined for the synthesis **51** to give **46** as an off-white solid (17 mg, 15% yield). ^{1}H NMR 500MHZ, $CDCl_3$ δ 3.06-3.11 (m, 4H), 3.63-3.67 (m, 4H), 5.15 (s, 2H), 6.74 (s, 1H), 6.79 (s, 1H), 7.37-7.41 (m, 1H), 7.55-7.58 (m, 2H), 7.96-7.99 (m, 1H), 8.26-8.28 (m, 1H), 8.64-8.67 (m, 1H), 8.77-8.80

(m, 1H). $[M+H]^+$ = 415.2. HRMS $[M+H]^+$ calculated for $C_{21}H_{21}Cl_2N_4O_1$ = 415.1087, found = 415.1079

*1-(4-(3,5-Dichloro-4-(pyridin-2-ylmethoxy)phenyl)pyridin-2-yl)piperazine (**47**).* Prepared using **42** (186 mg, 0.44 mmol, 1 eq), and pyridin-2-ylmethanol (58 mg, 0.53 mmol, 1.2 eq), according to the Mitsunobu reaction and BOC deprotection procedure outlined for the synthesis **51** to give **47** as an off-white solid (130 mg, 71% yield). ^{1}H NMR 500MHz, $CDCl_3$ δ 3.04-3.06 (m, 4H), 3.60-3.63 (m, 4H), 5.25 (s, 2H), 6.74 (d, *J* = 5.29 Hz, 1H), 6.78 (s, 1H), 7.29 (d, *J* = 1.26 Hz, 2H), 7.30-7.32 (m, 1H), 7.80-7.86 (m, 2H), 8.27 (d, *J* = 5.25 Hz, 1H), 8.63 (d, *J* = 4.30 Hz, 1H). $[M+H]^+$ = 415.1. HRMS $[M+H]^+$ calculated for $C_{21}H_{21}Cl_2N_4O_1$ = 415.1087, found = 415.1088

*1-(4-(3,5-Dichloro-4-((2,6-dimethylpyridin-3-yl)methoxy)phenyl)pyridin-2-yl)piperazine (**48**).* Prepared using **42** (200 mg, 0.44 mmol, 1 eq), and (2,6-dimethylpyridin-3-yl)methanol (**43**) (for synthesis see Supporting Information) (78 mg, 0.57 mmol, 1.2 eq), according to the Mitsunobu reaction and BOC deprotection procedure outlined for the synthesis **51** to give **48** as an off-white solid (130 mg, 63% yield). ^{1}H NMR 500MHz, $CDCl_3$ δ 2.59 (s, 3H), 2.72 (s, 3H), 3.0-3.07 (m, 4H), 3.60-3.63 (m, 4H), 5.11 (s, 2H), 6.74 (s, 1H), 6.78 (d, *J* = 5.27 Hz, 1H), 7.07 (d, *J* = 7.81 Hz, 1H), 7.57 (s, 2H), 7.76 (d, *J* = 7.81 Hz, 1H), 8.27 (d, *J* = 5.16 Hz, 1H). $[M+H]^+$ = 443.1. HRMS $[M+H]^+$ calculated for $C_{23}H_{25}Cl_2N_4O_1$ = 443.14, found = 443.1402

*1-(4-(3,5-Dichloro-4-((2,4-dimethylpyridin-3-yl)methoxy)phenyl)pyridin-2-yl)piperazine) (**49**).* Prepared using **42** (112 mg, 0.28 mmol, 1 eq), and (2,6-dimethylpyridin-4-yl)methanol (**44**) (for synthesis see Supporting Information) (44 mg, 0.32 mmol, 1.2 eq), according to the Mitsunobu reaction and BOC deprotection procedure outlined for the synthesis **51** to give **49** as an off-white solid (56 mg, 49% yield). ^{1}H NMR 500MHz, DMSO δ 2.44 (s, 3H), 2.68 (s,

3H), 2.93-2.99 (m, 4H), 3.60-3.68 (m, 4H), 5.24 (s, 2H), 7.00 (d, *J* = 5.20 Hz, 1H), 7.10-7.14 (m, 2H), 7.96 (s, 2H), 8.16 (d, *J* = 5.1 Hz, 1H), 8.29 (d, *J* = 5.13 Hz, 1H). $[M+H]^+$ = 443.2. HRMS $[M+H]^+$ calculated for $C_{23}H_{25}Cl_2N_4O_1$ = 443.1400, found = 443.1392

*1-(4-(3,5-Dichloro-4-(2-(pyridin-2-yl)ethoxy)phenyl)pyridin-2-yl)piperazine (**50**)*. Prepared using **42** (120 mg, 0.28 mmol, 1 eq), and 2-(2-hydroxyethyl)pyridine (38 µL, 0.34 mmol, 1.2 eq), according to the Mitsunobu reaction and BOC deprotection procedure outlined for the synthesis **51** to give **50** as an off-white solid (24 mg, 20% yield). ^{1}H NMR 500MHz, $CDCl_3$ δ 3.02-3.05 (m, 4H), 3.39 (t, *J* = 6.75 Hz, 2H), 3.58-3.61 (m, 4H), 4.49 (t, *J* = 6.65 Hz, 2H), 6.71 (s, 1H), 6.75 (dd, *J* = 1.50 Hz, 5.25, 1H), 7.18-7.21 (m, 1H), 7.39 (d, *J* = 7.93 Hz, 1H), 7.51 (s, 2H), 7.65-7.69 (m, 1H), 8.25 (dd, *J* = 0.64, 5.25 Hz, 1H), 8.58-8.60 (m, 1H). $[M+H]^+$ = 429.1. HRMS $[M+H]^+$ calculated for $C_{22}H_{23}Cl_2N_4O_1$ = 429.1243, found = 429.1231

*1-(4-(3,5-Dichloro-4-(2-(pyridin-4-yl)ethoxy)phenyl)pyridin-2-yl)piperazine) (**52**)*. Prepared using **42** (112 mg, 0.28 mmol, 1 eq) and 4-(2-hydroxyethyl)pyridine (42 mg, 0.34 mmol, 1.2eq) according to the Mitsunobu reaction and BOC deprotection procedure outlined for the synthesis **51** to give **52** as an off-white solid (22 mg, 18% yield). ^{1}H NMR 500MHz, $CDCl_3$ δ 3.02-3.05 (m, 4H), 3.22 (t, *J* = 6.68 Hz, 2H), 3.58-3.61 (m, 4H), 4.33 (t, *J* = 6.68 Hz, 2H), 6.71 (s, 1H), 6.75 (dd, *J* = 1.44 Hz, 5.25, 1H), 7.33 (dd, *J* = 1.59, 5.96 Hz, 2H), 7.53 (s, 2H), 8.25 (dd, *J* = 0.57, 5.19 Hz, 1H), 8.58 (dd, *J* = 1.54, 4.22 Hz, 2H). $[M+H]^+$ = 429.1. HRMS $[M+H]^+$ calculated for $C_{22}H_{23}Cl_2N_4O_1$ = 429.123956, found = 429.123956

Compounds **56-67** were synthesized using the standard Mitsunobu coupling conditions followed by BOC deprotection using TFA from **42** according to the procedure outlined in the synthesis of **51**. Or in the case of **56** using the methodology used for compound **29.**

*3-((2,6-Dichloro-4-(2-(piperazin-1-yl)pyridin-4-yl)phenoxy)methyl)-5-methylisoxazole dihydrochloride (**56**)*. 4-bromo-2,6-dichlorophenol (500 mg, 2.07 mmol, 1eq) and (5-methylisoxazol-3-yl)methanol (351 mg, 3.10 mmol, 1.5 eq) were reacted according to the

method outlined for **27** to give 3-((4-bromo-2,6-dichlorophenoxy)methyl)-5-methylisoxazole as a white solid (348 mg, 50% yield). ^{1}H NMR 500MHz, $CDCl_3$ δ 2.46 (d, *J* = 0.85 Hz, 3H), 5.08 (s, 2H), 6.28-6.29 (m, 1H), 7.48 (s, 2H). LCMS $[M+H]^+$ = 337.9.

3-((4-Bromo-2,6-dichlorophenoxy)methyl)-5-methylisoxazole (100 mg, 0.30 mmol, 1 eq) and **28** (86 mg, 0.30 mmol, 1 eq) were reacted according to the method outlined for the synthesis of **29** to give **56** as a dihydrochloride salt (104 mg, 71% yield. ^{1}H NMR 300MHz, DMSO δ 2.45 (s, 3H), 3.17-3.26 (m, 4H), 3.90-3.97 (m, 4H), 5.14 (s, 2H), 6.48-6.50 (m, 1H), 7.24 (d, *J* = 6.03Hz, 1H), 7.37-7.40 (m, 1H), 8.07 (s, 2H), 8.20 (d, *J* = 5.73Hz, 1H), 9.36 (br s, 2H). LCMS $[M+H]^+$ = 419.1. HRMS $[M+H]^+$ calculated for $C_{20}H_{21}N_4O_2Cl_2$ = 419.1042, found = 419.1032

*5-((2,6-Dichloro-4-(2-(piperazin-1-yl)pyridin-4-yl)phenoxy)methyl)-2,4-dimethylthiazole (**57**)*. Prepared using **42** (200 mg, 0.47 mmol, 1 eq), and (2,4-dimethyl-1,3-thiazol-5-yl)methanol (82 mg, 0.57 mmol, 1.2 eq), according to the Mitsunobu reaction and BOC deprotection procedure outlined for the synthesis of **51** to give **57** as an off-white solid (70 mg, 36% yield). ^{1}H NMR 500MHz, $CDCl_3$ δ 2.46 (s, 3H), 2.71 (s, 3H), 3.04-3.07 (m, 4H), 3.61-3.64 (m, 4H), 5.19 (s, 2H), 6.73 (s, 1H), 6.77 (d, *J* = 5.27, 1H), 7.56 (s, 2H), 8.26 (d, *J* = 5.27 Hz, 1H). $[M+H]^+$ = 449.0913. HRMS $[M+H]^+$ calculated for $C_{21}H_{23}Cl_2N_4O_1S_1$ = 449.0964, found = 449.0949

*5-((2,6-Dichloro-4-(2-(piperazin-1-yl)pyridin-4-yl)phenoxy)methyl)-2,4-dimethyloxazole (**58**)*. Prepared using **42** (120 mg, 0.28 mmol, 1 eq), and (2,4-dimethyloxazol-5-yl)methanol (**51**) (see Supporting Information for synthesis) (53 mg, 0.42 mmol, 1.5 eq), according to the Mitsunobu reaction and BOC deprotection procedure outlined for the synthesis of **51** to give **58** as an off-white solid (20 mg, 17% yield). ^{1}H NMR 500MHz, $CDCl_3$ δ 2.09 (s, 3H), 2.47 (s, 3H), 3.03-3.06 (m, 4H), 3.60-3.63 (m, 4H), 5.10 (s, 2H), 6.72 (s, 1H), 6.77 (dd, *J* = 1.28,

5.11 Hz, 1H), 7.54 (s, 2H), 8.26 (d, *J* = 5.18 Hz, 1H). $[M+H]^+$ = 433.2. HRMS $[M+H]^+$ calculated for $C_{21}H_{23}Cl_2N_4O_2$ = 433.1193, found = 433.1200

*4-((2,6-Dichloro-4-(2-(piperazin-1-yl)pyridin-4-yl)phenoxy)methyl)-2,5-dimethyloxazole (**59**)*. Prepared using **42** (120 mg, 0.28 mmol, 1 eq), and (2,5-dimethyl-1,3-oxazol-4-yl)methanol (53 mg, 0.42 mmol, 1.5 eq), according to the Mitsunobu reaction and BOC deprotection procedure outlined in the synthesis of **51** to give **59** as an off-white solid (27 mg, 22% yield). ^{1}H NMR 500MHz, $CDCl_3$ δ 2.37 (s, 3H), 2.46 (s, 3H), 3.03-3.06 (m, 4H), 3.60-3.62 (m, 4H), 4.97 (s, 2H), 6.73 (s, 1H), 6.77 (dd, *J* = 1.53, 5.21 Hz, 1H), 7.55 (s, 2H), 8.26 (dd, *J* = 0.61, 5.21 Hz, 1H). $[M+H]^+$ = 433.1

*4-((2,6-Dichloro-4-(2-(piperazin-1-yl)pyridin-4-yl)phenoxy)methyl)-2-methylthiazole (**60**)*. Prepared using **42** (150 mg, 0.35 mmol, 1 eq), and 2-(2-methyl-1,3-thiazol-4-yl)methanol (54 mg, 0.42 mmol, 1.2 eq), according to the Mitsunobu reaction and BOC deprotection procedure outlined for the synthesis of **51** to give **60** as an off-white solid (15 mg, 10% yield). ^{1}H NMR 500MHz, $CDCl_3$ δ 2.77 (s, 3H), 3.03-3.06 (m, 4H), 3.60-3.62 (m, 4H), 5.22 (s, 2H), 6.74 (s, 1H), 6.77 (dd, *J* = 1.45, 5.10 Hz, 1H), 7.37 (s, 1H), 7.56 (s, 2H), 8.26 (d, *J* = 5.22 Hz, 1H). $[M+H]^+$ = 435.1

*2-((2,6-Dichloro-4-(2-(piperazin-1-yl)pyridin-4-yl)phenoxy)methyl)thiazole (**61**)*. Prepared using **42** (120 mg, 0.28 mmol, 1 eq), and 2-(hydroxymethyl)-1,3-thiazole (48 mg, 0.42 mmol, 1.5 eq), according to the Mitsunobu reaction and BOC deprotection procedure outlined in the synthesis of **51** to give **61** as an off-white solid (24 mg, 20% yield). ^{1}H NMR 500MHz, $CDCl_3$ δ 3.03-3.06 (m, 4H), 3.60-3.62 (m, 4H), 5.44 (s, 2H), 6.73 (s, 1H), 6.77 (dd, *J* = 1.41, 5.14 Hz, 1H), 7.48 (d, *J* = 3.30 Hz, 1H), 7.57 (s, 2H), 7.86 (d, *J* = 3.30 Hz, 1H), 8.27 (d, *J* = 3.30 Hz, 1H). $[M+H]^+$ = 423.1. HRMS $[M+H]^+$ calculated for $C_{19}H_{19}Cl_2N_4O_1S_1$ = 421.0651, found = 421.0641

*4-((2,6-Dichloro-4-(2-(piperazin-1-yl)pyridin-4-yl)phenoxy)methyl)thiazole (**62**)*. Prepared using **42** (120 mg, 0.28 mmol, 1 eq), and 4-(hydroxymethyl)1,3-thiazole (48 mg, 0.42 mmol, 1.5 eq), according to the Mitsunobu reaction and BOC deprotection procedure outlined for the synthesis of **51** to give **62** as an off-white solid (5 mg, 4% yield). ^{1}H NMR 500MHz, $CDCl_3$ δ 3.03-3.06 (m, 4H), 3.60-3.62 (m, 4H), 5.34 (s, 2H), 6.74 (s, 1H), 6.78 (dd, *J* = 1.47, 5.23 Hz, 1H), 7.57 (s, 2H), 7.62-7.63 (m, 1H), 8.27 (dd, *J* = 0.68, 5.13 Hz, 1H), 8.87 (d, *J* = 2.09 Hz, 1H). $[M+H]^+$ = 423.1

*5-((2,6-Dichloro-4-(2-(piperazin-1-yl)pyridin-4-yl)phenoxy)methyl)-4-methylthiazole (**63**)*. Prepared using **42** (120 mg, 0.28 mmol, 1 eq), and (4-methylthiazol-5-yl)methanol (**52**) (for synthesis see Supporting Information) (54 mg, 0.42 mmol, 1.5 eq), according to the Mitsunobu reaction and BOC deprotection procedure outlined for the synthesis of **51** to give **63** as an off-white solid (9 mg, 7% yield). ^{1}H NMR 500MHz, $CDCl_3$ δ 2.56 (s, 3H), 3.03-3.06 (m, 4H), 3.60-3.63 (m, 4H), 5.28 (s, 2H), 6.73 (s, 1H), 6.77 (dd, *J* = 1.46, 5.19 Hz, 1H), 7.57 (s, 2H), 8.27 (dd, *J* = 0.6, 5.19 Hz, 1H), 8.79 (s, 1H). $[M+H]^+$ = 435.1. HRMS $[M+H]^+$ calculated for $C_{20}H_{21}Cl_2N_4O_1S_1$ = 435.0808, found = 435.0809

*5-((2,6-Dichloro-4-(2-(piperazin-1-yl)pyridin-4-yl)phenoxy)methyl)-2-ethyl-4-methylthiazole (**64**)*. Prepared using **42** (120 mg, 0.28 mmol, 1 eq), and (2-ethyl-4-methyl-1,3-thiazol-5-yl)methanol (66 mg, 0.42 mmol, 1.5 eq), according to the Mitsunobu reaction and BOC deprotection procedure outlined for the synthesis of **51** to give **64** as an off-white solid (26 mg, 20 % yield). ^{1}H NMR 500MHz, $CDCl_3$ δ 1.41 (t, *J* = 7.81, 3H), 2.47 (s, 3H), 3.00-3.06 (m, 6H), 3.60-3.62 (m, 4H), 5.19 (s, 2H), 6.73 (s, 1H), 6.77 (dd, *J* = 1.42, 5.20 Hz, 1H), 7.56 (s, 2H), 8.26 (d, *J* = 5.13 Hz, 1H). $[M+H]^+$ = 463.1. HRMS $[M+H]^+$ calculated for $C_{22}H_{25}Cl_2N_4O_1S_1$ = 463.1121, found = 463.1124

*5-((2,6-Dichloro-4-(2-(piperazin-1-yl)pyridin-4-yl)phenoxy)methyl)thiazole (**65**)*. Prepared using **42** (120 mg, 0.28 mmol, 1eq), and 5-(hydroxymethyl)-1,3-thiazole (48 mg, 0.42 mmol,

1.5 eq), according to the Mitsunobu reaction and BOC deprotection procedure outlined for the synthesis of **51** to give **65** as an off-white solid (23 mg, 20% yield). ^{1}H NMR 500MHz, $CDCl_3$ δ 3.06-3.08 (m, 4H), 3.64-3.66 (m, 4H), 5.33 (s, 2H), 6.73 (s, 1H), 6.78 (dd, *J* = 1.45, 5.20 Hz, 1H), 7.56 (s, 2H), 7.96 (s, 1H), 8.27 (d, *J* = 5.37 Hz, 1H), 8.90 (s, 1H). $[M+H]^+$ = 421.1, 423.1. HRMS $[M+H]^+$ calculated for $C_{19}H_{19}Cl_2N_4O_1S_1$ = 421.0651, found = 421.064

*5-((2,6-Dichloro-4-(2-(piperazin-1-yl)pyridin-4-yl)phenoxy)methyl)-2-isopropyl-4-methylthiazole (**66**).* Prepared using **42** (120 mg, 0.28 mmol, 1 eq), and (2-isopropyl-4-methylthiazol-5-yl)methanol (**53**) (for synthesis see Supporting Information) (73 mg, 0.42 mmol, 1.5 eq), according to the Mitsunobu reaction and BOC deprotection procedure outlined for the synthesis of **51** to give **66** as an off-white solid (37 mg, 28% yield). ^{1}H NMR 500MHz, $CDCl_3$ δ 1.42 (d, *J* = 7.12 Hz, 6H), 2.48 (s, 2H), 3.03-3.06 (m, 4H), 3.31 (sept, *J* = 6.97 Hz, 1H), 3.60-3.63 (m, 4H), 5.19 (s, 2H), 6.73 (s, 1H), 6.77 (dd, *J* = 1.36, 5.23 Hz, 1H), 7.57 (s, 2H), 8.27 (dd, *J* = 0.68, 5.23 Hz, 1H). $[M+H]^+$ = 477.2. HRMS $[M+H]^+$ calculated for $C_{23}H_{27}Cl_2N_4O_1S_1$ = 477.1277, found = 477.1273

*4-((2,6-Dichloro-4-(2-(piperazin-1-yl)pyridin-4-yl)phenoxy)methyl)-2-isopropylthiazole (**67**).* Prepared using **42** (120 mg, 0.28 mmol, 1 eq), and 4-(hydroxymethyl)-2-isopropylthiazole (66 mg, 0.42 mmol, 1.5 eq), according to the Mitsunobu reaction and BOC deprotection procedure outlined for the synthesis of **51** to give **67** as an off-white solid (1 mg, 1% yield). ^{1}H NMR 500MHz, $CDCl_3$ δ 1.43 (d, *J* = 6.85 Hz, 6H), 3.03-3.05 (m, 4H), 3.36 (sept, *J* = 6.95 Hz, 1H), 3.60-3.62 (m, 4H), 5.26 (s, 2H), 6.74 (s, 1H), 6.78 (dd, *J* = 1.47, 5.18 Hz, 1H), 7.55 (s, 2H), 8.26 (d, *J* = 5.12 Hz, 1H). $[M+H]^+$ = 463.1

*3-((2,6-Dichloro-4-(3-(piperidin-4-yl)propyl)phenoxy)methyl)-2-methylpyridine (**70**).* To a solution of tert-butyl 4-(but-3-en-1-yl)piperidine-1-carboxylate (0.58 g, 2.4 mmol, 2 eq) under argon in anhydrous THF (1ml) was added 9-BBN (5.1 ml (0.5 M in THF), 2.55 mmol, 2.1 eq) and reaction heated to 90 ^{o}C for 1 h in a microwave. To this crude reaction 3-((4-

bromo-2,6-dichlorophenoxy)methyl)-2-methylpyridine (0.42 g, 1.2 mmol, 1 eq), K_3PO_4 (1 M in H_2O, 2.4 mmol, 2.4 ml, 2 eq), in anhydrous DMF (2.5 ml) was added and then degassed with argon. $(Pd(PPh_3)_4$ (0.024 mmol, 28 mg, 2%) was then added and the solution microwaved at 110 ^oC for 1 h. The reaction was extracted into dichloromethane, washed with water and dried over $MgSO_4$. The crude material was purified by flash column chromatography, running a gradient from 0% ethyl acetate in hexane to 50% ethyl acetate in hexane. The Boc protected **70** was taken up in dichloromethane (12 mL), trifluoroacetic acid added (6 mL) and the reaction stirred for 2 h. The solvent was removed *in vacuo* to give a crude residue, which was purified by SCX-2, eluting with methanol to 2 M methanolic ammonia, followed by column chromatography, eluting with dichloromethane to dichloromethane:methanol (80:20) with 1% NH_3 to give **70** (0.105g, 10%) as an oil. ^1H NMR 500 MHz, $CDCl_3$ δ 1.05 - 1.13 (m, 2H), 1.23 - 1.40 (m, 5H), 1.58 - 1.62 (m, 7H), 2.57 (dd, *J* = 7.7, 7.7 Hz, 2H), 2.70 (s, 3H), 4.07 - 4.10 (m, 2H), 5.05 (s, 2H), 7.16 (s, 2H), 7.21 (dd, *J* = 4.9, 7.6 Hz, 1H), 7.90 (dd, *J* = 1.5, 7.6 Hz, 1H), 8.52 (dd, *J* = 1.7, 4.9 Hz, 1H). HRMS $[M+H]^+$ calculated for $C_{22}H_{23}Cl_2N_4O$ = 429.124343, found = 429.124407

*3-((2,6-Dichloro-4-(3-(1-methylpiperidin-4-yl)propyl)phenoxy)methyl)-2-methylpyridine (**71**).* 3-((2,6-Dichloro-4-(3-(piperidin-4-yl)propyl)phenoxy)methyl)-2-methylpyridine (**70**) (0.07 g, 0.17 mmol, 1 eq) was taken up in chloroform (10 mL), treated with paraformaldehyde (0.052 g, 10 eq) and heated at 55 ^oC for 1 h. The reaction mixture was then treated with sodium triacetoxyborohydride (0.183 g, 0.86 mmol, 5 eq) and heating continued for 16 h. The reaction mixture was cooled to room temperature, and then partitioned between dichloromethane and sodium bicarbonate solution. The dichloromethane layer was separated and dried over $MgSO_4$ and solvent removed. The crude material was purified by column chromatography, eluting with dichloromethane to dichloromethane:methanol (95:5) with 1% NH_3 to give (**71**) as a white solid (58 mg, 76% yield). ^1H NMR 500 MHz, $CDCl_3$ δ 1.23 -

1.30 (m, 5H), 1.34 - 1.39 (m, 2H), 1.87 - 1.92 (m, 2H), 2.27 (s, 3H), 2.56 (dd, *J* = 7.8, 7.8 Hz, 2H), 2.70 (s, 4H), 2.85 (d, *J* = 11.3 Hz, 2H), 5.05 (s, 2H), 5.33 (s, 1H), 7.16 (s, 2H), 7.21 (dd, *J* = 5.1, 7.6 Hz, 1H), 7.90 (dd, *J* = 1.6, 7.6 Hz, 1H), 8.52 (dd, *J* = 1.7, 4.8 Hz, 1H). $[M+H]^+$ = 421.1889. HRMS $[M+H]^+$ calculated for $C_{23}H_{31}Cl_2N_2O_1$ = 421.1808, found = 421.1802

*Ethyl 2-chloronicotinate (**72**) and ethyl 2-ethoxynicotinate (**75**)*. To a suspension of 2-chloronicotinic acid (4.6 g, 29.2 mmol) in ethanol (50 mL), conc H_2SO_4 (2 mL) was added dropwise and the suspension heated to reflux for 3 h to form a solution. Reaction then cooled and evaporated *in vacuo*, then carefully neutralized with sat. aq. $NaHCO_3$ and extracted into ethyl acetate. The organic layer was washed with water and then dried over $MgSO_4$, filtered, absorbed onto silica and purified using flash column chromatography running a gradient from 0% ethyl acetate/hexane to 50% ethyl acetate/hexane to give the title compounds (ethyl 2-chloronicotinate **72**, bottom spot, 2.33 g, 43% yield and ethyl 2-ethoxynicotinate **75**, top spot, 923 mg, 16% yield). Ethyl 2-chloronicotinate (**72**) ^{1}H NMR 500MHz, $CDCl_3$ δ 1.45 (t, *J* = 7.61 Hz, 3H), 4.45 (q, *J* = 7.07 Hz, 2H), 7.36 (dd, *J* = 4.76, 7.71 Hz, 1H), 8.19 (dd, *J* = 2.09, 7.87 Hz, 1H), 8.54 (dd, *J* = 2.09, 4.77 Hz, 1H). $[M+H]^+$ = 186.1. Ethyl 2-ethoxynicotinate (**75**) ^{1}H NMR 500MHz, $CDCl_3$ δ 1.14 (t, *J* = 7.06 Hz, 3H), 1.47 (t, *J* = 6.92 Hz, 3H), 4.39 (q, *J* = 7.20 Hz, 2H), 4.50 (q, *J* = 7.06 Hz, 2H), 6.94 (dd, *J* = 4.98, 7.48 Hz, 1H), 8.16 (dd, *J* = 2.01, 7.48 Hz, 1H), 8.30 (dd, *J* = 2.01, 4.88 Hz, 1H). $[M+H]^+$ = 196.1

Prototypical Negishi Reaction between a chloropyridine and alkylzinc bromide

*Ethyl 2-isobutylnicotinate (**74a**)*. Anhydrous THF (9 mL) was added to a flame dried argon purged flask containing ethyl 2-chloronicotinate (**72**) (227 mg, 1.2 mmol, 1 eq) and $Pd(^tBuP)_2$ (31 mg, 0.06 mmol, 5%) and the mixture stirred until clear. To this isobutylzinc bromide (0.5 M in THF, 2.6 mL, 1.3 mmol, 1.1 eq) was added dropwise and the resulting solution heated at 60 ^{o}C overnight. The reaction was absorbed onto silica and eluted to remove baseline

material before purifying again by flash column chromatography using 25% ethyl acetate/hexane as the eluent to give **74a** as a yellow oil (164 mg, 66% yield). ^{1}H NMR 500MHz, $CDCl_3$ δ 0.95 (d, *J* = 6.75 Hz, 6H), 1.43 (t, *J* = 7.25 Hz, 3H), 2.13 (sept, *J* = 6.75 Hz, 1H), 3.11 (d, *J* = 7.25 Hz, 2H), 4.41 (q, *J* = 7.13 Hz, 2H), 8.16 (dd, *J* = 1.88, 7.75 Hz, 1H), 8.67 (dd, *J* = 1.88, 4.75 Hz, 1H). [M+H] = 208.

Prototypical Suzuki reaction of a chloropyridine and boronic acid

*Ethyl 2-phenylnicotinate (**73**)* A solution of ethyl 2-chloronicotinate (**72**) (793 mg, 4.3 mmol, 1 eq), phenylboronic acid (773 mg, 6.4 mmol, 1.5 eq) in 1M aq. K_3PO_4 (4 mL) and dioxane (6 mL) in a microwave vessel was degassed with argon for 5 min before addition of $Pd(PPh_3)_4$ (64 mg, 0.055 mmol, 5%), and degassing again for a further 5 min before microwaving at 140 ^{o}C for 15 min. The reaction mixture was partitioned between dichloromethabe and aq. sat. $NaHCO_3$, and the organic layer absorbed onto silica and purified by flash column chromatography running a gradient from 0% ethyl acetate/hexane to 25% ethyl acetate/hexane, affording **73** as an oil (927 mg, 95% yield). ^{1}H NMR 500MHz, $CDCl_3$ δ 1.07 (t, *J* = 7.19 Hz, 3H), 4.18 (q, *J* = 7.19 Hz, 2H), 7.37 (dd, *J* = 4.91, 7.87 Hz, 1H), 7.45-7.48 (m, 3H), 7.55-7.57 (m, 2H), 8.14 (dd, *J* = 1.71, 7.76 Hz, 1H), 8.79 (dd, *J* = 1.83, 4.78 Hz, 1H). [M+H] = 228.2

Prototypical pyridyl ester reduction to an alcohol

*(2-iso-Butylpyridin-3-yl)methanol (**77a**).* To a solution of ethyl 2-iso-butylnicotinate **74a** (774 mg, 3.7 mmol, 1 eq) in anhydrous THF (5 mL) at 0 ^{o}C, 0.5 M $LiAlH_4$ in THF (5.6 mL, 11.2 mmol, 3 eq) was added dropwise and the solution allowed to warm to room temperature before being stirred at RT for 16 h. Sodium sulfite decahydrate was added to the solution, the reaction diluted with dichloromethane and allowed to stir for 30 min. The reaction was filtered, the filtrate layers separated, the organic layer dried over $MgSO_4$ and evaporated *in*

vacuo to give **77a** as a yellow oil (452 mg, 74% yield). ^{1}H NMR 500MHz, $CDCl_3$ δ 0.97 (d, *J* = 6.67, 6H), 2.19 (sept, *J* = 6.82 Hz, 1H), 2.71 (d, *J* = 7.42 Hz, 2H), 4.79 (d, *J* = 5.51 Hz, 2H), 7.17 (dd, *J* = 4.78, 7.82 Hz, 1H), 7.60 (d, *J* = 7.68 Hz, 1H), 8.50 (dd, *J* = 1.74, 4.78 Hz, 1H). [M+H] = 166.2

*1-(4-(3,5-Dichloro-4-((2-ethoxypyridin-3-yl)methoxy)phenyl)pyridin-2-yl)piperazine (**79**)*. Prepared using **42** (200 mg, 0.47 mmol, 1 eq), and (2-ethoxypyridin-3-yl)methanol (**78**) (87 mg, 0.57 mmol, 1.2 eq), according to the Mitsunobu reaction and BOC deprotection procedure outlined for the synthesis of **51** to give **79** as an off-white solid (30 mg, 33% yield). ^{1}H NMR 500MHz, $CDCl_3$ δ 1.42 (t, *J* = 7.21 Hz, 3H), 2.66-2.69 (m, 4H), 3.65-3.68 (m, 4H), 4.41 (q, *J* = 7.07 Hz, 2H), 6.72 (dd, *J* = 1.42, 5.21 Hz, 1H), 6.90 (dd, *J* = 5.04, 7.20 Hz, 1H), 7.53 (s, 1H), 7.72 (dd, *J* = 1.61, 7.50 Hz, 1H), 8.09 (dd, *J* = 1.96, 5.04 Hz, 1H), 8.24 (d, *J* = 5.24 Hz, 1H). [M+H] = 459.2. HRMS $[M+H]^+$ calculated for $C_{23}H_{25}Cl_2N_4O_2$ = 459.1349, found = 459.1339

*4-(3-((2,6-Dichloro-4-(2-(piperazin-1-yl)pyridin-4-yl)phenoxy)methyl)pyridin-2-yl)morpholine (**80**)*. Prepared using **42** (200 mg, 0.47 mmol, 1 eq), and (2-morpholinopyridin-3-yl)methanol (110 mg, 0.57 mmol, 1.2 eq), according to the Mitsunobu reaction and BOC deprotection procedure outlined for the synthesis of **51** to give **80** as an off-white solid (58 mg, 28% yield). ^{1}H NMR 500MHz, $CDCl_3$ δ 3.04-3.06 (m, 4H), 3.28-3.31 (m, 4H), 3.60-3.63 (m, 4H), 3.88-3.90 (m, 4H), 5.15 (s, 2H), 6.74 (s, 1H), 6.79 (dd, *J* = 1.48, 5.29 Hz, 1H), 7.60 (s, 2H), 8.07 (dd, *J* = 1.93, 7.51 Hz, 1H), 8.28 (d, *J* = 5.23 Hz, 1H), 8.37 (dd, *J* = 1.93, 4.89 Hz, 1H). $[M+H]^+$ = 500.2. HRMS $[M+H]^+$ calculated for $C_{25}H_{28}Cl_2N_5O_2$ = 500.161457, found = 500.160771

*1-(4-(3,5-Dichloro-4-((2-isobutylpyridin-3-yl)methoxy)phenyl)pyridin-2-yl)piperazine (**81**)*. Prepared using **42** (200 mg, 0.47 mmol, 1 eq), and (2-isobutylpyridin-3-yl)methanol (**77a**) (94 mg, 0.57 mmol, 1.2 eq), according to the Mitsunobu reaction and BOC deprotection

procedure outlined for the synthesis **51** to give **81** as an off-white solid (86 mg, 40% yield). ^{1}H NMR 500MHz, $CDCl_3$ δ 1.00 (d, *J* = 6.69 Hz, 6H), 2.23 (sept, *J* = 6.91 Hz, 1H), 3.04-3.06 (m, 4H), 3.60-3.63 (m, 4H), 5.14 (s, 2H), 6.74 (s, 1H), 6.78 (dd, *J* = 1.44, 5.11 Hz, 1H), 7.23 (dd, *J* = 4.75, 7.63 Hz, 1H), 7.59 (s, 2H), 7.98 (dd, *J* = 1.73, 7.77 Hz, 1H), 8.28 (dd, *J* = 0.65, 5.18 Hz, 1H), 8.60 (dd, *J* = 1.82, 4.86 Hz, 1H). $[M+H]^+$ = 471.2. HRMS $[M+H]^+$ calculated for $C_{25}H_{29}Cl_2N_4O_1$ = 471.1713, found = 471.1718

*1-(4-(3,5-Dichloro-4-((2-phenylpyridin-3-yl)methoxy)phenyl)pyridin-2-yl)piperazine (**82**)*. Prepared using **42** (200 mg, 0.47 mmol, 1 eq), and (2-phenylpyridin-3-yl)methanol **76** (for synthesis see Supporting Information) (105 mg, 0.57 mmol, 1.2 eq), according to the Mitsunobu reaction and BOC deprotection procedure outlined in the synthesis of **51** to give **82** as an off-white solid (122 mg, 53% yield). ^{1}H NMR 500MHz, $CDCl_3$ δ 3.03-3.05 (m, 4H), 3.60-3.62 (m, 4H), 5.14 (s, 2H), 6.71 (s, 1H), 6.76 (dd, *J* = 1.44, 5.24 Hz, 1H), 7.41 (dd, *J* = 4.76, 7.68 Hz, 1H), 7.45-7.51 (m, 3H), 7.53 (s, 2H), 7.65-7.67 (m, 2H), 8.22 (dd, *J* = 1.65, 7.82 Hz, 1H), 8.26 (d, *J* = 5.21 Hz, 1H), 8.74 (dd, *J* = 1.71, 4.78 Hz, 1H). $[M+H]^+$ = 491.2. HRMS $[M+H]^+$ calculated for $C_{27}H_{25}Cl_2N_4O_1$ = 491.14, found = 491.1405

*1-(4-(3,5-Dichloro-4-((2-propylpyridin-3-yl)methoxy)phenyl)pyridin-2-yl)piperazine (**83**)*. Prepared using **42** (150 mg, 0.35 mmol, 1 eq), and (2-propylpyridin-3-yl)methanol (**77b**) (for synthesis see Supporting Information) (63 mg, 0.42 mmol, 1.2 eq), according to the Mitsunobu reaction and BOC deprotection procedure outlined for the synthesis of **51** to give **83** as an off-white solid (33 mg, 21% yield). ^{1}H NMR 500MHz, $CDCl_3$ δ 1.06 (t, *J* = 7.53 Hz, 3H), 1.79-1.87 (m, 2H), 2.96-2.99 (m, 2H), 3.04-3.06 (m, 4H), 3.60-3.63 (m, 4H), 5.14 (s, 2H), 6.74 (s, 1H), 6.78 (dd, *J* = 1.40, 5.20 Hz, 1H), 7.23 (dd, *J* = 4.86, 7.55 Hz, 1H), 7.59 (s, 2H), 7.95 (dd, *J* = 1.73, 7.66 Hz, 1H), 8.28 (dd, *J* = 0.70, 5.14 Hz, 1H), 8.59 (dd, *J* = 1.73, 4.87 Hz, 1H). $[M+H]^+$ = 457.2. HRMS $[M+H]^+$ calculated for $C_{24}H_{27}Cl_2N_4O_1$ = 457.1556, found = 457.1552

*1-(4-(3,5-Dichloro-4-((2-isopentylpyridin-3-yl)methoxy)phenyl)pyridin-2-yl)piperazine (**84**)*. Prepared using **42** (150 mg, 0.35 mmol, 1 eq), and (2-isopentylpyridin-3-yl)methanol (**77c**) (for synthesis see Supporting Information) (75 mg, 0.42 mmol, 1.2 eq), according to the Mitsunobu reaction and BOC deprotection procedure outlined for the synthesis of **51** to give **84** as an off-white solid (109 mg, 65% yield). ^{1}H NMR 500MHz, $CDCl_3$ δ 1.00 (d, J = 6.84 Hz, 6H), 1.65-1.72 (m, 2H), 1.73 (sept, J = 6.87 Hz, 1H), 2.97-3.01 (m, 2H), 3.03-3.06 (m, 4H), 3.60-3.63 (m, 4H), 5.14 (s, 2H), 6.74 (s, 1H), 6.78 (dd, J = 1.39, 5.16 Hz, 1H), 7.22 (dd, J = 4.79, 7.74 Hz, 1H), 7.58 (s, 2H), 7.95 (dd, J = 1.80, 7.70 Hz, 1H), 8.28 (dd, J = 0.61, 5.12 Hz, 1H), 8.58 (dd, J = 1.76, 4.92 Hz, 1H). $[M+H]^+$ = 485.2. HRMS $[M+H]^+$ calculated for $C_{26}H_{31}Cl_2N_4O_1$ = 485.1869, found = 485.1888

X-ray Crystallography Methods

*Af*NMT protein–ligand complexes were determined using methods described previously[30]. Ternary complexes of AfNMT with myristoyl CoA (MCoA) and ligands of interest were obtained by co-crystallisation by incubating protein with 10 mM MCoA plus 10 mM ligand diluted from a 100 mM stock in DMSO prior to crystallization. Diffraction data were measured at the European Synchrotron Radiation Facility (ESRF). Data integration and scaling was carried out using XDS[36] and AIMLESS[37] or the HKL suite[38]. Structures were phased by molecular replacement with MOLREP[39] from the CCP4 suite[40] using the protein coordinates of *Af*NMT:compound **1**, (PDB 4CAX) as a search model. Refinement was carried out using REFMAC5[41] and manual model alteration was carried out using Coot[42]. Ligand-coordinate and restraint files were generated using PRODRG[43] and ligands were modelled into unbiased F_{obs} - F_{calc} density maps using Coot

Coordinates for *Af*NMT–ligand complexes and associated diffraction data have been

deposited in the RCSB Protein Data Bank (PDB) with accession codes 5T5U, 5T6C, 5T6E and 5T6H for compounds **24**, **29**, **48** and **49** respectively. Data measurement and refinement statistics are shown in Supplemental Information.

NMT enzyme assay

NMT assays [44-45] were carried out at room temperature (22–23 °C) in 384-well white optiplates (Perkin Elmer). Each assay was performed in a 40 µL reaction volume containing 30 mM Tris buffer, pH 7.4, 0.5 mM EDTA, 0.5 mM EGTA, 1.25 mM dithiothreitol (DTT), 0.1% (v/v) Triton X-100, 0.125 µM [^{3}H]myristoyl-coA (8 Curie (Ci) mmol^{-1}), 0.5 µM biotinylated CAP5.5, 5 nM NMT and various concentrations of the test compound. The IC_{50} values for *Hs*NMT1 and *Hs*NMT2 were essentially identical against 80 compounds tested and, for logistical reasons, only *Hs*NMT1 was used in later studies.

Test compound (0.4 µl in DMSO) was transferred to all assay plates using a Cartesian Hummingbird (Genomics Solution) before 20 µl of enzyme was added to assay plates. The reaction was initiated with 20 µl of a substrate mix and stopped after 15 min (HsNMT1 or HsNMT2) or 50 min (TbNMT) with 40 µl of a stop solution containing 0.2 M phosphoric acid, pH 4.0 and 1.5 M $MgCl_2$ and 1 mg ml^{-1} PVT SPA beads (GE Healthcare). All reaction mix additions were carried out using a Thermo Scientific WellMate (Matrix). Plates were sealed and read on a TopCount NXT Microplate Scintillation and Luminescence Counter (Perkin Elmer).

ActivityBase from IDBS was used for data processing and analysis. All IC_{50} curve fitting was undertaken using XLFit version 4.2 from IDBS. A four-parameter logistic dose response curve was used using XLFit 4.2 Model 205. All test compound curves had floating top and bottom and pre-fit was used for all four parameters.

Compound efficacy and trypanocidal activity in cultured *T. brucei* parasites

Bloodstream *T. b. brucei* s427 were cultured at 37 °C in modified HMI9 medium (56 μM 1-thioglycerol was substituted for 200 μM 2-mercaptoethanol) and quantified using a haemocytometer. For the live/dead assay, cells were analysed using a two-colour cell viability assay (Invitrogen) as described previously[22]. Cell culture plates were stamped with 1 μL of an appropriate concentration of test compound in DMSO followed by the addition of 200 μL trypanosome culture (10^4 cells ml^{-1}) to each well, except for one column which received media only. MRC-5 cells were cultured in DMEM, seeded at 2,000 cells per well and allowed to adhere overnight. One-microlitre of test compound (10 point dilutions from 50 μM to 2 nM) was added to each well at the start of the assay. Culture plates of *T. brucei* and MRC-5 cells were incubated at 37 °C in an atmosphere of 5% CO_2 for 69 h, before the addition of 20 μL resazurin (final concentration, 50 μM). After a further 4 h incubation, fluorescence was measured (excitation 528 nm; emission 590 nm) using a BioTek flx800 plate reader.

ASSOCIATED CONTENT

Supporting information

Experimental details for compounds **3** – **12** and **17** – **24**

X-ray data collection and refinement statistics

Correlation of enzyme activity data for inhibitors against *Af*NMT and *Tb*NMT

Molecular structures on known NMT ihibitors

Molecular formulas strings for compounds described in this paper are available

Corresponding Author Information

Paul G. Wyatt *Phone +44-(0)1382 386 231; E-mail p.g.wyatt@dundee.ac.uk

Notes

The authors declare no competing financial interest.

ACKNOWLEDGEMNTS

Funding for this work was provided by the Wellcome Trust (Grant Ref. WT077705 and Strategic Award WT083481). We would like to thank Gina McKay for performing HRMS analyses and Daniel James for data management. We thank the European Synchrotron Radiation Facility (ESRF) for synchrotron beamtime and support, and Paul Fyfe for supporting the in-house X-ray facility.

ABBREVIATIONS USED

NMT, *N*-Myristoyltransferase; *T. brucei, Trpanosoma brucei*; *T. br. brucei, T. brucei. brucei*; HAT, human African trypanosomiasis or sleeping sickness; CNS, central nervous system; *Tb*NMT, *T. brucei* N-myristoyltransferase; *Hs*NMT, human NMT; LE, Ligand Efficiency; PSA, polar surface area, *Af*NMT, *Aspergillus fumigatus* NMT; HBA, hydrogen bond acceptor; HBD, hydrogen bond donor; BBB, blood-brain barrier; MW, molecular weight; cLogP, calculated LogP, cLogD, calculated LogD; SAR, structure activity relationship; nd, not determined.

References

1. Pink, R.; Hudson, A.; Mouries, M. A.; Bendig, M. Opportunities and challenges in antiparasitic drug discovery. *Nat. Rev. Drug Discovery* **2005,** *4*, 727-740.

2. WHO Trypanosomiasis, Human African trypanosomiasis (sleeping sickness). http://www.who.int/mediacentre/factsheets/fs259/en/., accessed October 15, 2017

3. Brun, R.; Balmer, O. New developments in human African trypanosomiasis. *Curr. Opin. Infect. Dis* **2006,** *19*, 415-420.

4. Kennedy, P. G. The continuing problem of human African trypanosomiasis (sleeping sickness). *Ann. Neurol.* **2008,** *64*, 116-126.

5. Wery, M. Drug used in the treatment of sleeping sickness (human African trypanosomiasis: HAT). *Int. J. Antimicrob. Agents* **1994,** *4*, 227-238.

6. Jacobs, R. T.; Nare, B.; Phillips, M. A. State of the art in African trypanosome drug discovery. *Curr. Top. Med. Chem.* **2011,** *11,* 1255-1274.

7. Frearson, J. A.; Brand, S.; McElroy, S. P.; Cleghorn, L. A.; Smid, O.; Stojanovski, L.; Price, H. P.; Guther, M. L.; Torrie, L. S.; Robinson, D. A.; Hallyburton, I.; Mpamhanga, C. P.; Brannigan, J. A.; Wilkinson, A. J.; Hodgkinson, M.; Hui, R.; Qiu, W.; Raimi, O. G.; van Aalten, D. M.; Brenk, R.; Gilbert, I. H.; Read, K. D.; Fairlamb, A. H.; Ferguson, M. A.; Smith, D. F.; Wyatt, P. G. N-myristoyltransferase inhibitors as new leads to treat sleeping sickness. *Nature* **2010,** *464*, 728-732.

8. Hertz-Fowler, C.; Ersfeld, K.; Gull, K. CAP5.5, a life-cycle-regulated, cytoskeleton-associated protein is a member of a novel family of calpain-related proteins in Trypanosoma brucei. *Mol. Biochem. Parasitol.* **2001,** *116*, 25-34.

9. Price, H. P.; Panethymitaki, C.; Goulding, D.; Smith, D. F. Functional analysis of TbARL1, an N-myristoylated Golgi protein essential for viability in bloodstream trypanosomes. *J. Cell. Sci.* **2005,** *118*, 831-841.

10. Price, H. P.; Stark, M.; Smith, D. F. Trypanosoma brucei ARF1 plays a central role in endocytosis and golgi-lysosome trafficking. *Mol. Biol. Cell.* **2007,** *18*, 864-873.

11. Price, H. P.; Guther, M. L.; Ferguson, M. A.; Smith, D. F. Myristoyl-CoA:protein N-myristoyltransferase depletion in trypanosomes causes avirulence and endocytic defects. *Mol. Biochem. Parasitol.* **2010,** *169*, 55-58.

12. Price, H. P.; Menon, M. R.; Panethymitaki, C.; Goulding, D.; McKean, P. G.; Smith, D. F. Myristoyl-CoA:protein N-myristoyltransferase, an essential enzyme and potential drug target in kinetoplastid parasites. *J. Biol. Chem.* **2003,** *278*, 7206-7214.

13. Farazi, T. A.; Waksman, G.; Gordon, J. I. The biology and enzymology of protein N-myristoylation. *J. Biol. Chem.* **2001,** *276*, 39501-39504.

14. Wright, M. H.; Clough, B.; Rackham, M. D.; Rangachari, K.; Brannigan, J. A.; Grainger, M.; Moss, D. K.; Bottrill, A. R.; Heal, W. P.; Broncel, M.; Serwa, R. A.; Brady, D.; Mann, D. J.; Leatherbarrow, R. J.; Tewari, R.; Wilkinson, A. J.; Holder, A. A.; Tate, E. W. Validation of N-myristoyltransferase as an antimalarial drug target using an integrated chemical biology approach. *Nat. Chem.* **2014,** *6*, 112-121.

15. Wright, M. H.; Paape, D.; Storck, E. M.; Serwa, R. A.; Smith, D. F.; Tate, E. W. Global analysis of protein N-myristoylation and exploration of N-myristoyltransferase as a drug target in the neglected human pathogen Leishmania donovani. *Chem. Biol.* **2015,** *22*, 342-354.

16. Herrera, L. J.; Brand, S.; Santos, A.; Nohara, L. L.; Harrison, J.; Norcross, N. R.; Thompson, S.; Smith, V.; Lema, C.; Varela-Ramirez, A.; Gilbert, I. H.; Almeida, I. C.; Maldonado, R. A. Validation of N-myristoyltransferase as Potential Chemotherapeutic Target in Mammal-Dwelling Stages of Trypanosoma cruzi. *PLoS Neglected Trop. Dis.* **2016,** *10*, e0004540.

17. Roberts, A. J.; Fairlamb, A. H. The N-myristoylome of Trypanosoma cruzi. *Sci. Rep.* **2016,** *6*, 31078.

18. Ritzefeld, M.; Wright, M. H.; Tate, E. W. New developments in probing and targeting protein acylation in malaria, leishmaniasis and African sleeping sickness. *Parasitology* **2017**, 1-18.

19. Rampoldi, F.; Bonrouhi, M.; Boehm, M. E.; Lehmann, W. D.; Popovic, Z. V.; Kaden, S.; Federico, G.; Brunk, F.; Grone, H. J.; Porubsky, S. Immunosuppression and aberrant T cell development in the absence of N-myristoylation. *J. Immunol.* **2015,** *195*, 4228-4243.

20. Das, U.; Kumar, S.; Dimmock, J. R.; Sharma, R. K. Inhibition of protein N-myristoylation: a therapeutic protocol in developing anticancer agents. *Curr. Cancer Drug Targets* **2012,** *12*, 667-692.

21. Thinon, E.; Morales-Sanfrutos, J.; Mann, D. J.; Tate, E. W. N-Myristoyltransferase Inhibition Induces ER-Stress, Cell Cycle Arrest, and Apoptosis in Cancer Cells. *ACS Chem. Biol.* **2016,** *11*, 2165-2176.

22. Brand, S.; Cleghorn, L. A.; McElroy, S. P.; Robinson, D. A.; Smith, V. C.; Hallyburton, I.; Harrison, J. R.; Norcross, N. R.; Spinks, D.; Bayliss, T.; Norval, S.; Stojanovski, L.; Torrie, L. S.; Frearson, J. A.; Brenk, R.; Fairlamb, A. H.; Ferguson, M. A.; Read, K. D.; Wyatt, P. G.; Gilbert, I. H. Discovery of a novel class of orally active trypanocidal N-myristoyltransferase inhibitors. *J. Med. Chem.* **2012,** *55*, 140-152.

23. Brand, S. W., P.; Thompson, S.; Smith, V.; Bayliss, T.; Harrison, J.; Norcross, N.; Cleghorn, L.; Gilbert, I.; Brenk, R. N-Myristoyl transferase inhibitors. Patent WO2010026365. 2010.

24. Brand, S.; Norcross, N. R.; Thompson, S.; Harrison, J. R.; Smith, V. C.; Robinson, D. A.; Torrie, L. S.; McElroy, S. P.; Hallyburton, I.; Norval, S.; Scullion, P.; Stojanovski, L.; Simeons, F. R. C.; van Aalten, D.; Frearson, J. A.; Brenk, R.; Fairlamb, A. H.; Ferguson, M. A. J.; Wyatt, P. G.; Gilbert, I. H.; Read, K. D. Lead optimization of a pyrazole sulfonamide series of Trypanosoma brucei N-myristoyltransferase inhibitors: Identification and evaluation of CNS penetrant compounds as potential treatments for stage 2 human african trypanosomiasis. *J. Med. Chem.* **2014,** *57*, 9855-9869.

25. Hopkins, A. L.; Groom, C. R.; Alex, A. Ligand efficiency: a useful metric for lead selection. *Drug Discovery Today* **2004,** *9*, 430-431.

26. Ebiike, H.; Masubuchi, M.; Liu, P.; Kawasaki, K.; Morikami, K.; Sogabe, S.; Hayase, M.; Fujii, T.; Sakata, K.; Shindoh, H.; Shiratori, Y.; Aoki, Y.; Ohtsuka, T.; Shimma, N. Design and synthesis of novel benzofurans as a new class of antifungal agents targeting fungal N-myristoyltransferase. Part 2. *Bioorg. Med. Chem. Lett.* **2002,** *12*, 607-610.

27. Masubuchi, M.; Kawasaki, K.; Ebiike, H.; Ikeda, Y.; Tsujii, S.; Sogabe, S.; Fujii, T.; Sakata, K.; Shiratori, Y.; Aoki, Y.; Ohtsuka, T.; Shimma, N. Design and synthesis of novel benzofurans as a new class of antifungal agents targeting fungal N-myristoyltransferase. Part 1. *Bioorg. Med. Chem. Lett.* **2001,** *11*, 1833-1837.

28. Sogabe, S.; Masubuchi, M.; Sakata, K.; Fukami, T. A.; Morikami, K.; Shiratori, Y.; Ebiike, H.; Kawasaki, K.; Aoki, Y.; Shimma, N.; D'Arcy, A.; Winkler, F. K.; Banner, D. W.; Ohtsuka, T. Crystal structures of Candida albicans N-myristoyltransferase with two distinct inhibitors. *Chem. Biol.* **2002,** *9*, 1119-1128.

29. Armour, D. R.; Bell., A. S.; Kemp, M. I.; Edwards, M. P.; Wood, A. Discovery of a novel series of non-peptidic fungal N-myristoyl transferase inhibitors. 221st ACS National Meeting, San Diego, CA, United States, April 1-5, 2001; pp MEDI-349.

30. Fang, W.; Robinson, D. A.; Raimi, O. G.; Blair, D. E.; Harrison, J. R.; Lockhart, D. E.; Torrie, L. S.; Ruda, G. F.; Wyatt, P. G.; Gilbert, I. H.; van Aalten, D. M. N-myristoyltransferase is a cell wall target in Aspergillus fumigatus. *ACS Chem. Biol.* **2015,** *10*, 1425-1434.

31. Patani, G. A.; LaVoie, E. J. Bioisosterism: A rational approach in drug design. *Chem. Rev.* **1996,** *96*, 3147-3176.

32. Clark, D. E. In silico prediction of blood-brain barrier permeation. *Drug Discovery Today* **2003,** *8*, 927-933.

33. Hitchcock, S. A.; Pennington, L. D. Structure-brain exposure relationships. *J. Med. Chem.* **2006,** *49*, 7559-7583.

34. Yu, Z.; Brannigan, J. A.; Moss, D. K.; Brzozowski, A. M.; Wilkinson, A. J.; Holder, A. A.; Tate, E. W.; Leatherbarrow, R. J. Design and synthesis of inhibitors of Plasmodium falciparum N-myristoyltransferase, a promising target for antimalarial drug discovery. *J. Med. Chem.* **2012,** *55*, 8879-8890.

35. Shultz, M. D. Setting expectations in molecular optimizations: Strengths and limitations of commonly used composite parameters. *Bioorg. Med. Chem. Lett.* **2013,** *23*, 5980-5991.

36. Kabsch, W. Xds. *Acta Crystallogr. Sect. D: Biol. Crystallogr.* **2010,** *66* (Pt 2), 125-32.

37. Evans, P. R.; Murshudov, G. N. How good are my data and what is the resolution? *Acta Crystallogr. D: Biol. Crystallogr.***2013,** *69*, 1204-1214.

38. Otwinowski, Z.; Minor, W. Processing of X-ray diffraction data collected in oscillation mode. In *Methods in Enzyemology*, Carter Jr, C. W.; Sweet, R. M., Eds. 1997; Vol. 276, pp 307-326.

39. Vagin, A.; Teplyakov, A. Molecular replacement with MOLREP. *Acta Crystallogr. Sect. D: Biol. Crystallogr.* **2010,** *66*, 22-25.

40. Winn, M. D.; Ballard, C. C.; Cowtan, K. D.; Dodson, E. J.; Emsley, P.; Evans, P. R.; Keegan, R. M.; Krissinel, E. B.; Leslie, A. G.; McCoy, A.; McNicholas, S. J.; Murshudov, G. N.; Pannu, N. S.; Potterton, E. A.; Powell, H. R.; Read, R. J.; Vagin, A.; Wilson, K. S. Overview of the CCP4 suite and current developments. *Acta Crystallogr. Sect. D: Biol. Crystallogr.* **2011,** *67*, 235-242.

41. Murshudov, G. N.; Skubak, P.; Lebedev, A. A.; Pannu, N. S.; Steiner, R. A.; Nicholls, R. A.; Winn, M. D.; Long, F.; Vagin, A. A. REFMAC5 for the refinement of macromolecular crystal structures. *Acta Crystallogr. Sect. D: Biol. Crystallogr.* **2011,** *67*, 355-67.

42. Emsley, P.; Cowtan, K. Coot: model-building tools for molecular graphics. *Acta Crystallogr. Sect. D: Biol. Crystallogr.* **2004,** *60*, 2126-2132.

43. Schuttelkopf, A. W.; van Aalten, D. M. PRODRG: a tool for high-throughput crystallography of protein-ligand complexes *Acta Crystallogr. Sect. D: Biol. Crystallogr.***2004,** *60*, 1355-1363.

44. Bowyer, P. W.; Gunaratne, R. S.; Grainger, M.; Withers-Martinez, C.; Wickramsinghe, S. R.; Tate, E. W.; Leatherbarrow, R. J.; Brown, K. A.; Holder, A. A.; Smith, D. F. Molecules incorporating a benzothiazole core scaffold inhibit the N-myristoyltransferase of Plasmodium falciparum. *Biochem. J.* **2007,** *408*, 173-180.

45. Panethymitaki, C.; Bowyer, P. W.; Price, H. P.; Leatherbarrow, R. J.; Brown, K. A.; Smith, D. F. Characterization and selective inhibition of myristoyl-CoA:protein N-myristoyltransferase from Trypanosoma brucei and Leishmania major. *Biochem. J.* **2006,** *396*, 277-285.

Table of Contents graphic